

Maintaining gauge symmetry in renormalizing chiral gauge theories

Er-Cheng Tsai*

Physics Department, National Taiwan University, Taipei 10617, Taiwan

(Received 1 October 2010; revised manuscript received 13 December 2010; published 7 March 2011)

It is known that the γ_5 scheme of Breitenlohner and Maison in dimensional regularization requires finite counterterm renormalization to restore gauge symmetry and implementing this finite renormalization in practical calculation is a daunting task even at 1-loop order. In this paper, we show that there is a simple and straightforward method to obtain these finite counterterms by using the rightmost γ_5 scheme in which we move all the γ_5 matrices to the rightmost position before analytically continuing the dimension. For any 1-loop Feynman diagram, the difference between the amplitude regularized in the rightmost γ_5 scheme and the amplitude regularized in the Breitenlohner and Maison scheme can be easily calculated. The differences for all 1-loop diagrams in the chiral Abelian-Higgs gauge theory and in the chiral non-Abelian gauge theory are shown to be the same as the amplitudes due to the finite counterterms that are required to restore gauge symmetry.

DOI: 10.1103/PhysRevD.83.065011

PACS numbers: 11.10.Gh, 11.15.Bt, 11.30.Rd

I. INTRODUCTION

It is generally accepted that the original γ_5 dimensional regularization scheme proposed by 't Hooft and Veltman [1] and later systematized by Breitenlohner and Maison [2] can be used to regulate and renormalize chiral gauge theories in a rigorous manner. In this BM scheme, γ_5 is maintained as

$$\gamma_5 = i\gamma^0\gamma^1\gamma^2\gamma^3 \quad (1)$$

even when the space-time dimension n departs from 4. Such γ_5 anticommutes with γ^μ for μ in the first 4 dimensions but commutes with γ^μ when the index μ falls beyond the first 4 dimensions. As a consequence, an identity such as $\gamma_5\gamma^\mu = -\gamma^\mu\gamma_5$ in $n = 4$ dimensional space no longer holds under dimensional regularization when the polarization μ is continued beyond the first 4 dimensions. The continuation to $n \neq 4$ for the Lagrangian of a theory with a gauge invariant 4 dimensional Lagrangian, therefore, depends on how we express and continue the terms involving the product of γ_5 and γ^μ matrices in the Lagrangian. Furthermore, terms that are not gauge invariant in the n dimensional Lagrangian must vanish when $n \rightarrow 4$ and thus contain a factor of $(n - 4)$ or a γ^μ matrix with μ in the extra 4 dimensions. Such gauge variant evanescent terms will contribute to the violation of gauge symmetry in the perturbative calculation of the theory under dimensional regularization.

The breakdown of gauge symmetry in the Breitenlohner and Maison (BM) scheme can be remedied by introducing gauge variant local counterterms to restore the renormalized Ward identities [3] or BRST [4] gauge symmetry [5–9]. This procedure of removing spurious anomalies is usually a complicated and tedious task even at the 1-loop order. C. P. Martin and D. Sanchez-Ruiz [8] managed to

successfully calculate the 1-loop finite counterterms needed for restoring gauge symmetry of the chiral non-Abelian gauge theory. The 1-loop finite counterterms for the chiral Abelian-Higgs theory were later obtained by D. Sanchez-Ruiz [9] in which the laborious calculations were handled by computer routines.

In this paper, we shall present a simple and straightforward method for obtaining these finite counterterms. This is done with the help of the rightmost γ_5 scheme [10] in which the dimension n is analytically continued after all the γ_5 matrices have been moved to the rightmost position.

II. THE RIGHTMOST γ_5 SCHEME

For the QED theory, the identity

$$\frac{1}{\ell + k - m} k \frac{1}{\ell - m} = \frac{1}{\ell - m} - \frac{1}{\ell + k - m} \quad (2)$$

is the foundation that a Ward identity is built upon. For a gauge theory involving γ_5 , there is a basic identity similar to (2) for verifying Ward identities:

$$\begin{aligned} & \frac{1}{\ell + k - m} (k - 2m) \gamma_5 \frac{1}{\ell - m} \\ &= \gamma_5 \frac{1}{\ell - m} + \frac{1}{\ell + k - m} \gamma_5. \end{aligned} \quad (3)$$

The above identity, valid at $n = 4$, is derived by decomposing the vertex factor $(k - 2m)\gamma_5$ into $(\ell + k - m)\gamma_5$ and $\gamma_5(\ell - m)$ to annihilate, respectively, the propagators of the outgoing fermion with momentum $\ell + k$ and the incoming fermion with momentum ℓ . Positioning γ_5 at the rightmost site, (3) becomes

$$\begin{aligned} & \frac{1}{\ell + k - m} (k - 2m) \frac{1}{-\ell - m} \gamma_5 \\ &= \left(\frac{1}{-\ell - m} + \frac{1}{\ell + k - m} \right) \gamma_5. \end{aligned} \quad (4)$$

*ectsai@ntu.edu.tw

If we disregard the rightmost γ_5 on both sides of the above identity, we obtain another identity

$$\frac{1}{\ell + k - m}(k - 2m)\frac{1}{-\ell - m} = \frac{1}{-\ell - m} + \frac{1}{\ell + k - m} \quad (5)$$

that is valid at $n = 4$. This new identity (5), which is void of γ_5 , may be analytically continued to hold when $n \neq 4$. We then multiply γ_5 on the right to every analytically continued term of this γ_5 -free identity (5) to yield the analytic continuation of the identity (3).

As a side remark, we note that when we go to the dimension of $n \neq 4$, (3), in the form presented above, is not valid. This is because γ_5 does not always anticommute with γ^μ if $n \neq 4$. Adopting the rightmost γ_5 ordering avoids this difficulty, as the validity of the identity in the form of rightmost γ_5 ordering no longer depends on γ_5 anticommuting with the γ matrices.

Before analytic continuation is made, a γ_5 -odd (γ_5 -even) matrix product may always be reduced to a matrix product with only one (zero) γ_5 factor. For an amplitude corresponding to a diagram involving no fermion loops, we shall move all γ_5 matrices to the rightmost position before we continue analytically, the dimension n . The subsequent application of dimensional regularization gives us regulated amplitudes satisfying the Ward identities. An identity relating the traces of matrix products without γ_5 at $n = 4$ can always be analytically continued to hold when $n \neq 4$. Therefore, the portion of an amplitude in which the count of γ_5 on every fermion loop is even has no γ_5 difficulty and does not violate any Ward identity in this continuation scheme.

For any 1-loop Feynman diagram, the amplitude calculated according to the rightmost γ_5 scheme can be easily compared to that calculated according to the BM scheme. In fact, the difference between these two amplitudes can be straightforwardly calculated. If the rightmost γ_5 scheme is a gauge invariant scheme, we should be able to attribute the difference to the amplitude due to local counterterms that are required to restore BRST symmetry. It will be verified below with detailed results that this is indeed what happens. For the chiral Abelian-Higgs theory, the finite counterterms obtained by calculating the difference between the rightmost γ_5 scheme and the BM scheme are found to be exactly the same as those obtained in [9]. For the chiral non-Abelian gauge theory, the finite counterterms obtained in [8] can also be accounted for by the difference. These results serve to confirm that the rightmost γ_5 scheme is indeed a gauge invariant regularization scheme.

III. LAGRANGIAN FOR THE CHIRAL ABELIAN-HIGGS THEORY

The BRST invariant Lagrangian density for the chiral Abelian-Higgs gauge theory is

$$\begin{aligned} L_B = & -\frac{1}{4}F_{\mu\nu}F^{\mu\nu} + (D^\mu\phi)^\dagger(D_\mu\phi) \\ & -\frac{1}{2}\lambda g^2\left(\phi^\dagger\phi - \frac{1}{2}v^2\right)^2 + \bar{\psi}_L(i\not{D})\psi_L \\ & + \bar{\psi}_R(i\not{\partial})\psi_R - \sqrt{2}f(\bar{\psi}_L\phi\psi_R + \bar{\psi}_R\phi^\dagger\psi_L) \\ & -\frac{1}{2\alpha}(\partial_\mu A^\mu - \alpha\Lambda\phi_2)^2 + i\bar{c}(\partial_\mu\partial^\mu + \alpha\Lambda M)c \\ & + ig\alpha\Lambda\bar{c}Hc, \end{aligned} \quad (6)$$

where c is the ghost field, \bar{c} is the antighost field, and

$$\begin{aligned} F_{\mu\nu} & \equiv \partial_\mu A_\nu - \partial_\nu A_\mu, \\ D_\mu\phi & \equiv (\partial_\mu + igA_\mu)\phi, \\ \psi_L & = L\psi, \quad \psi_R = R\psi, \end{aligned}$$

with the chiral projection operators L and R defined as

$$L = \frac{1}{2}(1 - \gamma_5), \quad R = \frac{1}{2}(1 + \gamma_5).$$

The complex scalar field ϕ is related to real H and ϕ_2 by

$$\phi = \frac{H + i\phi_2 + v}{\sqrt{2}}. \quad (7)$$

The Lagrangian L_B of (6) is invariant under the BRST variations:

$$\begin{aligned} \delta_B A_\mu & = \partial_\mu c, \\ \delta_B \phi_2 & = -Mc - gcH, \\ \delta_B H & = gc\phi_2, \\ \delta_B \psi_L & = -igc\psi_L, \\ \delta_B \psi_R & = 0, \\ \delta_B \bar{c} & = -\frac{i}{\alpha}(\partial^\mu A_\mu - \alpha\Lambda\phi_2), \\ \delta_B c & = 0. \end{aligned} \quad (8)$$

We define two mass parameters M and m by

$$M = gv, \quad m = fv. \quad (9)$$

Both M and m will be regarded as zero order quantities in perturbation.

Let us introduce the notation \underline{p}^μ for the component of p^μ vector in the first 4 dimensions and the notation p_Δ^μ for the component in the remaining dimensions, i.e.,

$$p^\mu = \underline{p}^\mu + p_\Delta^\mu,$$

with

$$\begin{aligned} p_\Delta^\mu & = 0 \quad \text{if } \mu \in \{0, 1, 2, 3\}, \\ \underline{p}^\mu & = 0 \quad \text{if } \mu \notin \{0, 1, 2, 3\}. \end{aligned}$$

Likewise, the Dirac matrix γ^μ is decomposed as

$$\gamma^\mu = \underline{\gamma}^\mu + \gamma_\Delta^\mu,$$

with $\gamma_\Delta^\mu = 0$ when $\mu \in \{0, 1, 2, 3\}$ and $\underline{\gamma}^\mu = 0$ when $\mu \notin \{0, 1, 2, 3\}$. Since the definition (1) for γ_5 is valid even when the space-time dimension n departs from 4, we have

$$\gamma_5 \gamma^\mu + \gamma^\mu \gamma_5 = 2\gamma_\Delta^\mu \gamma_5. \quad (10)$$

The free term involving the fermion fields in (6) is equal to

$$\begin{aligned} & \bar{\psi}_L i \not{\partial} \psi_L + \bar{\psi}_R i \not{\partial} \psi_R - f v (\bar{\psi}_L \psi_R + \bar{\psi}_R \psi_L) \\ & = \bar{\psi} (i R \not{\partial} L + i L \not{\partial} R - m) \psi = \bar{\psi} (i \underline{\not{\partial}} - m) \psi, \end{aligned} \quad (11)$$

where

$$\underline{\not{\partial}} = \partial_\mu \underline{\gamma}^\mu = \partial_\mu \gamma^\mu - \partial_\mu \gamma_\Delta^\mu = \not{\partial} - \not{\partial}_\Delta.$$

The fermion propagator corresponding to the free Lagrangian (11) is

$$\frac{i}{\underline{p} - m},$$

which is independent of p_Δ , the component of the momentum p in the extra 4 dimensions and cannot be used for perturbative dimensional calculation.

To remedy this ill behavior, let us add the term

$$E_0 = \bar{\psi} i \not{\partial}_\Delta \psi = \bar{\psi}_R i \not{\partial} \psi_L + \bar{\psi}_L i \not{\partial} \psi_R \quad (12)$$

to the BRST invariant L_B of (6). The theory defined by the Lagrangian

$$L_{\text{eff}} = L_B + E_0 \quad (13)$$

will have a well-behaved free fermion propagator

$$\frac{i}{\not{p} - m}$$

and can be used to calculate amplitudes perturbatively under the BM dimensional regularization scheme. By doing so, we also incur a loss of the BRST symmetry since $\delta_B L_{\text{eff}} = \delta_B E_0 \neq 0$. Because E_0 vanishes as $n \rightarrow 4$, E_0 does not have any tree-level contribution. At one or more loop orders, simple $\frac{1}{n-4}$ pole factors or higher pole terms may arise from divergent loop integrals so that the contribution of E_0 cannot be neglected and additional local counterterms are required to restore the BRST symmetry.

For the Abelian theory with the Lagrangian (13), the propagators can be readily read off the free Lagrangian and vertex factors can be determined from the interaction terms in the Lagrangian. The propagators and vertices that are relevant to the 1-loop finite counterterm calculation are listed in Appendix A 1.

IV. DIFFERENCE BETWEEN THE RIGHTMOST γ_5 SCHEME AND THE BM SCHEME IN THE ABELIAN-HIGGS THEORY

To illustrate how the counterterm amplitude is evaluated by calculating the difference between the rightmost γ_5

scheme and the BM scheme for the chiral Abelian-Higgs theory, consider the fermion self-energy diagram:



The horizontal line signifies an internal fermion line and the wavy line is a vector meson line. The Feynman amplitude in the BM scheme is

$$\begin{aligned} \Gamma^{\text{BM}} &= (-ig)^2 \int \frac{d^n \ell}{(2\pi)^n} D(A^\mu, A^\nu; \ell) R \gamma^\mu L \frac{i}{\ell + \not{p} - m} R \gamma^\nu L \\ &= -ig^2 \int \frac{d^n \ell}{(2\pi)^n} D(A^\mu, A^\nu; \ell) \frac{R \gamma^\mu L (\ell + \not{p}) R \gamma^\nu L}{(\ell + p)^2 - m^2}, \end{aligned} \quad (15)$$

where ℓ is the momentum of the internal vector meson line and the external momentum p flowing into the fermion self-energy correction has only components in the first 4 dimensions. Anticommuting γ_5 to the rightmost position, we obtain the corresponding amplitude in the rightmost γ_5 scheme:

$$\Gamma^{\text{R5}} = -ig^2 \int \frac{d^n \ell}{(2\pi)^n} D(A^\mu, A^\nu; \ell) \frac{\gamma^\mu (\ell + \not{p}) \gamma^\nu L}{(\ell + p)^2 - m^2}. \quad (16)$$

Both (15) and (16) are linearly divergent. Since the difference $(\Gamma^{\text{R5}} - \Gamma^{\text{BM}})$ contains at least a factor of γ_Δ matrix in the extra 4 dimensions, terms that are convergent will not survive the $n \rightarrow 4$ limit. We are free to change the mass pole of any propagator in evaluating $(\Gamma^{\text{R5}} - \Gamma^{\text{BM}})$ because the terms neglected are proportional to the mass square difference and are therefore convergent by power counting. Furthermore, if we expand the amplitude in a Taylor series with respect the external momentum p , terms proportional to p^N with $N \geq 2$ are convergent and can be discarded in the difference between (15) and (16), i.e., we may substitute $-i \frac{(g^{\mu\nu} + (\alpha-1) \frac{\ell^\mu \ell^\nu}{\ell^2 - m^2})}{(\ell^2 - m^2)^2}$ for $D(A^\mu, A^\nu; \ell)$ and $\frac{1}{\ell^2 - m^2} (1 - \frac{2\ell \cdot p}{\ell^2 - m^2})$ for $\frac{1}{(\ell + p)^2 - m^2}$. The difference $(\Gamma^{\text{R5}} - \Gamma^{\text{BM}})$ after utilizing $R \gamma^\mu L = \underline{\gamma}^\mu L$, $R \gamma^\nu L = \underline{\gamma}^\nu L$, and $L \ell R = \underline{\ell} R$ can be written as

$$\begin{aligned} \lim_{n \rightarrow 4} (\Gamma^{\text{R5}} - \Gamma^{\text{BM}}) &= -g^2 \lim_{n \rightarrow 4} \int \frac{d^n \ell}{(2\pi)^n} \\ &\quad \times \frac{(g^{\mu\nu} + (\alpha-1) \frac{\ell^\mu \ell^\nu}{\ell^2 - m^2}) (1 - \frac{2\ell \cdot p}{\ell^2 - m^2})}{(\ell^2 - m^2)^2} \\ &\quad \times (\gamma^\mu (\ell + \not{p}) \gamma^\nu - \underline{\gamma}^\mu (\ell + \not{p}) \underline{\gamma}^\nu) L. \end{aligned} \quad (17)$$

The symmetric integrals

$$\begin{aligned} \int d^n \ell f(\ell^2) \ell^\mu \ell^\nu &= \frac{g^{\mu\nu}}{n} \int d^n \ell f(\ell^2) \ell^2, \\ \int d^n \ell f(\ell^2) \ell^\mu \ell^\nu \ell^\rho \ell^\sigma &= \frac{(g^{\mu\nu} g^{\rho\sigma} + g^{\mu\rho} g^{\nu\sigma} + g^{\mu\sigma} g^{\rho\nu})}{n(n+2)} \\ &\quad \times \int d^n \ell f(\ell^2) \ell^4, \end{aligned}$$

enable us to set

$$\begin{aligned} \int d^n \ell f(\ell^2) (\ell \cdot p) \ell &= \frac{1}{n} \int d^n \ell f(\ell^2) \ell^2 \not{p}, \\ \int d^n \ell f(\ell^2) \ell^\mu \ell^\nu (\ell \cdot p) \ell &= \frac{g^{\mu\nu} \not{p} + p^\mu \gamma^\nu + p^\nu \gamma^\mu}{n(n+2)} \\ &\quad \times \int d^n \ell f(\ell^2) \ell^4, \end{aligned}$$

and reduce (17) to

$$\begin{aligned} \lim_{n \rightarrow 4} (\Gamma^{\text{R5}} - \Gamma^{\text{BM}}) &= \frac{g^2}{6} \lim_{n \rightarrow 4} \int \frac{d^n \ell}{(2\pi)^n} \frac{(n-4)}{(\ell^2 - m^2)^2} (1 + 2\alpha) \not{p} L \\ &= -\frac{1}{(4\pi)^2} i \frac{g^2}{3} (1 + 2\alpha) \not{p} L, \end{aligned} \quad (18)$$

where we have also utilized the integral

$$\lim_{n \rightarrow 4} \int \frac{d^n \ell}{(2\pi)^n} \frac{(n-4)}{(\ell^2 - m^2)^2} = 4 \int \frac{d^4 \ell}{(2\pi)^4} \frac{m^2}{(\ell^2 - 1)^3} = \frac{-2i}{(4\pi)^2}.$$

In the BM scheme, this amplitude (18) can be accounted for by adding the counterterm

$$-\frac{1}{(4\pi)^2} \frac{g^2}{3} (1 + 2\alpha) \bar{\psi} R i \not{\partial} L \psi \quad (19)$$

to the Lagrangian (13).

The counterterm amplitude for any divergent 1-loop 1PI diagram can be similarly calculated. The diagrams that are responsible for all 1-loop counterterms are listed in Figs. 1–7 in Appendix A. The corresponding counterterm amplitudes are calculated and summarized in Tables IV, V, VI, VII, VIII, IX, and X.

V. 1-LOOP RESULTS FOR THE CHIRAL ABELIAN-HIGGS THEORY

For the chiral Abelian-Higgs theory, D. Sanchez-Ruiz [9] has successfully computed in the BM scheme the 1-loop finite counterterms that are required to restore the BRST symmetry by evaluating the terms that break the Slavnov-Taylor identities and then solving a linear system of 27 equations with 32 variables to find a solution. The calculation in [9] is rather cumbersome and has to be relied on computer routines. The general solution for the 1-loop finite counterterms is given by (30) of [9]

$$\hbar \tilde{S}_{\text{fct}}^{(1)} = -\sum_{i=1}^{32} \hbar \tilde{x}_{0,i}^{(1)} \tilde{e}_i + \hbar \sum_{l=1}^{11} c_l^{(1)} I_l, \quad (20)$$

where each I_l , $l = 1, 2, \dots, 11$ is BRST invariant and \tilde{e}_i , $i = 1, 2, \dots, 32$ given by (16) in [9] form a basis of the space of the integrated Lorentz scalar CP -invariant polynomials in the fields and their derivatives with maximal canonical dimension 4 and ghost number 0. A particular solution for the coefficients $\tilde{x}_{0,i}^{(1)}$ is given by (29) in [9] and tabulated in the 2nd columns of Tables I, II, and III. Counterterms that involve fermion fields are listed in Table I. Otherwise, they are listed in Tables II and III.

The theory defined by the L_{eff} of (13) corresponds to the theory of (5) in [9] with $\xi' = \alpha$, $\rho = -\alpha\Lambda$, $\theta = 0$, and $r = 1$. Correspondingly, the 3rd column of Table I is obtained from the 2nd column with the substitution $\xi' = \alpha$, $\rho = -\alpha\Lambda$, $\theta = 0$, and $r = 1$.

From Tables IV, V, VI, and VII, the sum of counterterms due to the diagrams from Figs. 1–4, obtained according to the method of evaluating the difference between the rightmost γ_5 scheme and the BM scheme is equal to

$$\begin{aligned} &\frac{1}{(4\pi)^2} \left[-\frac{g^2}{3} (1 + 2\alpha) \bar{\psi} R i \not{\partial} L \psi \right. \\ &\quad + \frac{1}{2} \alpha (M - \Lambda) f g \bar{\psi} \psi + \frac{1}{6} g^3 (7 + 5\alpha) \bar{\psi} R A L \psi \\ &\quad \left. + f^2 g \bar{\psi} A \gamma_5 \psi + \frac{\alpha g^2 f}{2} \bar{\psi} (H + i \phi_2 \gamma_5) \psi \right], \end{aligned} \quad (21)$$

which, after subtracting out the gauge invariant term,

TABLE I. Counterterms due to diagrams with open fermion lines are shown in the table.

\tilde{e}_i	$-(4\pi)^2 \tilde{x}_{0,i}^{(1)}$	$\xi' = \alpha, \rho = -\alpha\Lambda, \theta = 0, r = 1$	Rightmost γ_5 method
$\tilde{e}_{24} = \bar{\psi} \psi$	$-\frac{f[3\rho r + 4g^2\theta(1+\theta r)v(5+\xi')]}{6r}$	$\frac{1}{2} \alpha \Lambda f$	$-\frac{1}{2} \alpha \Lambda f g$
$\tilde{e}_{25} = \bar{\psi} i \not{\partial} L \psi$	0	0	0
$\tilde{e}_{26} = \bar{\psi} i \not{\partial} R \psi$	0	0	0
$\tilde{e}_{27} = \bar{\psi} A L \psi$	$-\frac{[-6f^2 r + g^2(2\theta + r + \theta^2 r)(5+\xi')]}{6}$	$f^2 - \frac{1}{6} g^2 (5 + \alpha)$	$-f^2 g + \frac{1}{6} g^3 (5 + \alpha)$
$\tilde{e}_{28} = \bar{\psi} A R \psi$	$\frac{f[-6f^2 + g^2\theta^2(5+\xi')]}{6}$	$-f^2$	$f^2 g$
$\tilde{e}_{29} = \bar{\psi} H \psi$	$-\frac{2}{3} f g^2 \theta (\theta + r)(5 + \xi')$	0	0
$\tilde{e}_{30} = \bar{\psi} \phi_2 \gamma_5 \psi$	0	0	0

TABLE II. Counterterms without A fields due to diagrams with a closed fermion loop are shown in the table.

\tilde{e}_i	$-(4\pi)^2 \tilde{x}_{0,i}^{(1)}$	Rightmost γ_5 method
$\tilde{e}_1 = H$	$-8f^4 v^3$	$-8f^4 v^3$
$\tilde{e}_2 = H^2$	$-12f^4 v^2$	$-12f^4 v^2$
$\tilde{e}_3 = (\phi_2)^2$	0	0
$\tilde{e}_4 = H^3$	$-8f^4 v$	$-8f^4 v$
$\tilde{e}_5 = H(\phi_2)^2$	0	0
$\tilde{e}_6 = H^4$	$-2f^4$	$-2f^4$
$\tilde{e}_7 = (\phi_2)^4$	$\frac{2}{3}f^4$	$\frac{2}{3}f^4$
$\tilde{e}_8 = H^2(\phi_2)^2$	0	0
$\tilde{e}_9 = (\partial_\mu H)(\partial^\mu H)$	0	0
$\tilde{e}_{10} = (\partial_\mu \phi_2)(\partial^\mu \phi_2)$	$-\frac{2}{3}f^2$	$-\frac{2}{3}f^2$

$$\frac{1}{(4\pi)^2} \left[-\frac{g^2}{3} (1 + 2\alpha) \bar{\psi} R (i\not{\partial} - g\not{A}) L \psi + \frac{\alpha g^2 f}{2} \bar{\psi} (H + v + i\phi_2 \gamma_5) \psi \right],$$

becomes

$$\frac{1}{(4\pi)^2} \left[-\frac{1}{2} \alpha \Lambda f g \bar{\psi} \psi + \left(\frac{1}{6} g^3 (5 + \alpha) - f^2 g \right) \bar{\psi} R A L \psi + f^2 g \bar{\psi} A R \psi \right]. \quad (22)$$

The above expression (22), decomposed as a linear combination of \tilde{e}_i , is listed under the column ‘‘rightmost γ_5 method’’ in Table I. The Lagrangian (13) is defined differently from that in [9]. The covariant derivative D_μ is defined as $D_\mu = \partial_\mu + igA_\mu$ for the theory (13) but as $D_\mu = \partial_\mu - iA_\mu$ in [9]. The vector field A in a counterterm expression obtained in [9] needs to be scaled to $-gA$ to be identified as the corresponding counterterm for the theory

TABLE III. Counterterms involving A fields due to diagrams with a closed fermion loop are shown in the table.

\tilde{e}_i	$-(4\pi)^2 \tilde{x}_{0,i}^{(1)}$	Rightmost γ_5 method
$\tilde{e}_{11} = \phi_2(\partial_\mu A^\mu)$	0	0
$\tilde{e}_{12} = A_\mu H(\partial^\mu \phi_2)$	0	0
$\tilde{e}_{13} = A_\mu \phi_2(\partial^\mu H)$	$-4f^2$	$4f^2 g$
$\tilde{e}_{14} = A_\mu A^\mu$	$-f^2 v^2$	$-f^2 g^2 v^2$
$\tilde{e}_{15} = A_\mu A^\mu H$	$-2f^2 v$	$-2f^2 g^2 v$
$\tilde{e}_{16} = A_\mu A^\mu H^2$	$-f^2$	$-f^2 g^2$
$\tilde{e}_{17} = A_\mu A^\mu (\phi_2)^2$	$-3f^2$	$-3f^2 g^2$
$\tilde{e}_{18} = (\partial_\mu A^\mu)^2$	$\frac{1}{6}$	$\frac{1}{6} g^2$
$\tilde{e}_{19} = F_{\mu\nu} F^{\mu\nu}$	0	0
$\tilde{e}_{20} = (A_\mu A^\mu)^2$	$\frac{1}{12}$	$\frac{1}{12} g^4$

of (13). There is a single vector A field in $\tilde{e}_{27} = \bar{\psi} A L \psi$ or $\tilde{e}_{28} = \bar{\psi} A R \psi$. As a consequence, multiplying $-g$ to the coefficient of either \tilde{e}_{27} or \tilde{e}_{28} under the 3rd column of Table I should give us the corresponding coefficient under the column ‘‘rightmost γ_5 method.’’ Furthermore, the counterterm proportional to $\tilde{e}_{24} = \bar{\psi} \psi$ actually stems from diagrams (d) and (e) of Fig. 1. The ratio of the coefficient of \tilde{e}_{24} for the theory of (13) over that obtained in [9] as shown in Table I is equal to $-g$ and can be accounted for by the ratio of vertex factors due to the single $\bar{\psi} - A - \psi$ vertex in each of the diagrams (d) and (e) of Fig. 1. Table I, in fact, shows that the 1-loop counterterms that involve fermion fields calculated by the rightmost γ_5 method are in agreement with those obtained in [9].

The 1-loop counterterms due to the diagrams without external fermion lines from Figs. 5–7 are summarized in Tables VIII, IX, and X. The total of these counterterms is

$$\frac{1}{(4\pi)^2} \left[4m^2 f^2 (\phi_2)^2 - \frac{4}{3} f^2 (\partial \phi_2)^2 - g^2 m^2 A^2 + \frac{1}{6} g^2 (\partial_\mu A_\nu)(\partial^\mu A^\nu) + 8f^3 m H (\phi_2)^2 - 2f g^2 m H A^2 + 4f^2 g \phi_2 (\partial_\mu H) A^\mu + 4f^4 H^2 (\phi_2)^2 + \frac{8}{3} f^4 (\phi_2)^4 - f^2 g^2 H^2 A^2 - 3f^2 g^2 (\phi_2)^2 A^2 + \frac{1}{12} g^4 (A^2)^2 \right] \quad (23)$$

and can be written as the sum of

$$\frac{1}{(4\pi)^2} \left[2f^4 ((H + v)^2 + (\phi_2)^2)^2 - 2f^4 v^4 + \frac{1}{12} g^2 F_{\mu\nu} F^{\mu\nu} \right] \quad (24)$$

and

$$\frac{1}{(4\pi)^2} \left[-2f^4 (H^4 + 4vH^3 + 6v^2H^2 + 4v^3H) + \frac{2}{3} f^4 (\phi_2)^4 - \frac{2}{3} f^2 (\partial \phi_2)^2 + \frac{1}{6} g^2 (\partial_\mu A^\mu)^2 - g^2 m^2 A^2 - 2f g^2 m H A^2 + 4f^2 g \phi_2 (\partial_\mu H) A^\mu - f^2 g^2 H^2 A^2 + \frac{1}{12} g^4 (A^2)^2 - 3f^2 g^2 (\phi_2)^2 A^2 \right]. \quad (25)$$

Equation (24) is gauge invariant and (25), expressed as a linear combination of \tilde{e}_i , is tabulated in Tables II and III under the column ‘‘rightmost γ_5 method’’ while the result from [9] is listed under the column $-(4\pi)^2 \tilde{x}_{0,i}^{(1)}$. Taking the $-g$ factor into consideration for each vector field A in comparing the counterterm expressions, the counterterms listed in Tables II and III obtained by the rightmost γ_5 method for the theory of (13) are in exact agreement with those obtained in [9].

VI. LAGRANGIAN FOR THE CHIRAL NON-ABELIAN GAUGE THEORY

The BRST invariant Lagrangian density for the chiral non-Abelian gauge theory is

$$\begin{aligned} \tilde{L}_B = & -\frac{1}{4}F_{\mu\nu}^a F^{a,\mu\nu} + \bar{\psi}_L i\not{D}\psi_L + \bar{\psi}_R i\not{\partial}\psi_R \\ & + i\bar{\psi}'_R i\not{D}\psi'_R + \bar{\psi}'_L i\not{\partial}\psi'_L - \frac{1}{2\alpha}(\partial^\mu A_\mu^a)(\partial^\nu A_\nu^a) \\ & + i\bar{c}^a \square c^a + igC^{abc}(\partial^\mu \bar{c}^a)A_\mu^b c^c, \end{aligned} \quad (26)$$

where c^a is the ghost field, \bar{c}^a is the antighost field, and

$$F_{\mu\nu}^a = \partial_\mu A_\nu^a - \partial_\nu A_\mu^a - gC^{abc}A_\mu^b A_\nu^c.$$

Two fermion fields ψ and ψ' whose left-handed component $\psi_L = L\psi$ and right-handed component $\psi'_R = R\psi'$ are coupled to A_μ^a . The covariant derivatives for ψ_L and ψ'_R are

$$\begin{aligned} D_\mu \psi_L &= (\partial_\mu + igA_\mu^a T_L^a)\psi_L, \\ D_\mu \psi'_R &= (\partial_\mu + igA_\mu^a T_R^a)\psi'_R, \end{aligned}$$

where T_L^a (T_R^a) are group generators that satisfy

$$\begin{aligned} [T_L^a, T_L^b] &= iC^{abc}T_L^c, & [T_R^a, T_R^b] &= iC^{abc}T_R^c \\ \text{tr}(T_L^a T_L^b) &= T_L \delta^{ab}, & \text{tr}(T_R^a T_R^b) &= T_R \delta^{ab} \\ \sum_e T_L^e T_L^e &= C_L, & \sum_e T_R^e T_R^e &= C_R. \end{aligned}$$

For convenience, we also adopt the following shorthand notations defined in [8]:

$$\text{tr}(T_L^a T_L^b T_L^c T_L^d) = T_L^{abcd}, \quad \text{tr}(T_R^a T_R^b T_R^c T_R^d) = T_R^{abcd}.$$

The Lagrangian (26) is invariant under the BRST variations:

$$\begin{aligned} \delta_B A_\mu^a &= \partial_\mu c^a + gC^{abc}c^b A_\mu^c, \\ \delta_B \psi_L &= -ic^a T_L^a \psi_L, & \delta_B \psi_R &= 0, \\ \delta_B \psi'_R &= -ic^a T_R^a \psi'_R, & \delta_B \psi'_L &= 0, \\ \delta_B c^a &= \frac{1}{2}gC^{abc}c^b c^c, \\ \delta_B \bar{c}^a &= \frac{1}{i\alpha} \partial_\mu A^{a,\mu}. \end{aligned}$$

As with the chiral Abelian-Higgs theory (13), a gauge variant evanescent term

$$\tilde{E}_0 = \bar{\psi} i\not{\partial}_\Delta \psi + \bar{\psi}' i\not{\partial}_\Delta \psi' \quad (27)$$

needs to be added to the BRST invariant (26) to define the Lagrangian

$$\tilde{L}_{\text{eff}} = \tilde{L}_B + \tilde{E}_0 \quad (28)$$

for the chiral non-Abelian gauge theory that can be calculated perturbatively in the BM scheme. For the

non-Abelian theory (28), the propagators and vertices that are relevant to 1-loop finite counterterm calculation are listed in Appendix B 1.

VII. 1-LOOP RESULTS FOR THE CHIRAL NON-ABELIAN GAUGE THEORY

C.P. Martin and D. Sanchez-Ruiz have obtained with tedious calculations the 1-loop finite counterterms that are needed for restoring BRST symmetry in the BM dimensional regularization formalism for the chiral non-Abelian gauge theory with the result given in (69) of [8]. In Appendix B, the 1-loop counterterms for this non-Abelian theory are computed straightforwardly by evaluating the difference of amplitudes between the rightmost γ_5 scheme and the BM scheme with the results summarized in Table XI. Specifically, diagrams in Figs. 8 and 9 yield the counterterms that involve fermion fields and can be written as

$$\begin{aligned} & \frac{1}{(4\pi)^2} \left[-\frac{1}{3}g^2(1+2\alpha)(\bar{\psi}_L i\not{\partial}\psi_L C_L + \bar{\psi}'_R i\not{\partial}\psi'_R C_R) \right. \\ & \left. + \frac{1}{6}g^3(7+5\alpha)(\bar{\psi}_L A^a T_L^a \psi_L C_L + \bar{\psi}'_R A^a T_R^a \psi'_R C_R) \right]. \end{aligned} \quad (29)$$

Subtracting out the gauge invariant term

$$\begin{aligned} & \frac{1}{(4\pi)^2} \left[-i\frac{1}{6}g^2(7+5\alpha)(\bar{\psi}_L (\not{\partial} + igA^a T_L^a)\psi_L C_L \right. \\ & \left. + \bar{\psi}'_R (\not{\partial} + igA^a T_R^a)\psi'_R C_R \right] \end{aligned}$$

from (29), we get

$$\frac{1}{(4\pi)^2} \left[\left(1 + \frac{(\alpha-1)}{6} \right) g^2 (\bar{\psi}_L i\not{\partial}\psi_L C_L + \bar{\psi}'_R i\not{\partial}\psi'_R C_R) \right], \quad (30)$$

which, after the identification of α with α' , is consistent with the finite counterterms (69) of [8].

Figures 10–12 are responsible for the counterterms that are free of fermion fields. From Table XI, the sum of these counterterms is equal to

$$\begin{aligned} & \frac{1}{(4\pi)^2} \left[-\frac{1}{6}g^2(T_L + T_R)A_\mu^a \square A^{a,\mu} - \frac{2}{3}g^3(T_L + T_R) \right. \\ & \times C^{abc}(\partial^\mu A_\nu^a)A_\mu^b A^{c,\nu} + \frac{1}{12}g^4(T_L^{abcd} + T_R^{abcd}) \\ & \times A^{a,\mu}A_\mu^b A^{c,\nu}A_\nu^d + \frac{5}{24}g^4(T_L + T_R) \\ & \left. \times C^{eab}C^{ecd}A_\mu^a A_\nu^b A^{c,\mu}A^{d,\nu} \right], \end{aligned} \quad (31)$$

which can be written as the sum of the gauge invariant term

$$\frac{5}{24}g^2(T_L + T_R)F_{\mu\nu}^a F^{a,\mu\nu}$$

and

$$\frac{1}{(4\pi)^2} \left[\begin{array}{l} (T_L + T_R)g^2 \left(\frac{5}{12} (\partial A)^2 + \frac{1}{4} A \square A \right) \\ + \frac{(T_L + T_R)}{6} g^3 C^{abc} (\partial_\mu A_\nu^a) A_\mu^b A_\nu^c \\ + \frac{1}{12} g^4 (T_L^{abcd} + T_R^{abcd}) A^{a,\mu} A_\mu^b A^{c,\nu} A_\nu^d \end{array} \right]. \quad (32)$$

Upon the scaling of $A \rightarrow -gA$, the chiral non-Abelian gauge theory with the tree action defined by (32) in [8] becomes the non-Abelian theory defined by (26). Taking the $A \rightarrow -gA$ scaling into consideration, (32) is also in agreement with (69) of [8].

VIII. CONCLUSION

In the BM scheme, simply removing the pole terms from the amplitudes of 1-loop diagrams does not yield renormalized amplitudes that satisfy Ward identities. Instead, some finite renormalization terms have to be added. These finite counterterms are determined from restoring the validities of Ward identities. Implementing this finite renormalization in practical calculation is usually a daunting task even at 1-loop order.

For the chiral Abelian-Higgs gauge theory and the chiral non-Abelian Yang-Mills theory, we have verified that the renormalized amplitudes for all 1-loop diagrams calculated in the BM scheme with finite counterterm renormalization

are equal to those obtained directly in the rightmost γ_5 scheme. This means we can be spared the tedious finite renormalization procedures if the rightmost γ_5 scheme is adopted. Furthermore, since all the γ_5 matrices are moved to and consolidated at a single position before continuing the dimension in our scheme, the burden of evaluating the matrix products or trace of matrix products is considerably less than that in the BM scheme. In our opinion, this rightmost γ_5 prescription is a much simpler scheme than the BM scheme for calculating amplitudes in gauge theories involving γ_5 .

For the rightmost γ_5 scheme, the prescription that leads to the preservation of Ward identities makes no use of the specific type of gauge theories in question. As a consequence, the rightmost γ_5 scheme should be applicable for any type of chiral gauge theory, in particular, the standard model.

APPENDIX A: THE CHIRAL ABELIAN-HIGGS THEORY

1. Feynman rules

The propagators and vertices used in the 1-loop counterterm calculation for the chiral Abelian-Higgs theory defined by (13) are listed below.

a. Propagators

$$S(\psi, \bar{\psi}; p) : \begin{array}{c} p \\ \longleftarrow \\ \hline \end{array} = \frac{i}{\not{p} - m}$$

$$D(A^\mu, A^\nu; k) : \begin{array}{c} \longleftarrow k \\ \text{~~~~~} \\ \mu \quad \nu \end{array} = -i \left(\frac{g^{\mu\nu} - \frac{k^\mu k^\nu}{k^2}}{k^2 - M^2} + \frac{\alpha(k^2 - \alpha\Lambda^2) k^\mu k^\nu}{k^2 (k^2 - \alpha\Lambda M)^2} \right)$$

$$D(A^\mu, \phi_2; k) : \begin{array}{c} \longleftarrow k \\ \text{~~~~~} \\ \mu \quad \phi_2 \end{array} = \frac{\alpha(M - \Lambda) k^\mu}{(k^2 - \alpha\Lambda M)^2}$$

$$D(\phi_2, A^\mu; k) : \begin{array}{c} \longleftarrow k \\ \phi_2 \quad \text{~~~~~} \\ \mu \end{array} = -\frac{\alpha(M - \Lambda) k^\mu}{(k^2 - \alpha\Lambda M)^2}$$

$$D(\phi_2, \phi_2; k) : \begin{array}{c} \longleftarrow k \\ \phi_2 \quad \text{~~~~~} \\ \phi_2 \end{array} = \frac{i(k^2 - \alpha M^2)}{(k^2 - \alpha\Lambda M)^2}$$

$$D(H, H; k) : \begin{array}{c} \longleftarrow k \\ \text{~~~~~} \\ H \quad H \end{array} = \frac{i}{k^2 - \lambda M^2}$$

b. Vertex factors

$$\bar{\psi} A^\mu \psi : \text{---} \left(\text{---} \overset{\mu}{\text{wavy}} \text{---} \right) \text{---} = -igR\gamma^\mu L$$

$$\bar{\psi} \phi_2 \psi : \text{---} \left(\text{---} \overset{\phi_2}{\text{vertical}} \text{---} \right) \text{---} = f(R-L) = f\gamma_5$$

$$\bar{\psi} H \psi : \text{---} \left(\text{---} \overset{H}{\text{vertical}} \text{---} \right) \text{---} = -if$$

$$H A^\mu \phi_2 : \begin{array}{c} k \\ \text{wavy} \\ \mu \\ \text{---} \text{---} \\ \text{---} \text{---} \\ p+k \quad H \quad \phi_2 \quad p \end{array} = g(2p^\mu + k^\mu)$$

2. 1-Loop counterterms

a. Figure 1: $\bar{\psi}\psi$ self-energy diagrams

The possible diagrams that may contribute to the fermion self-energy are depicted in Fig. 1.

In each diagram of Fig. 1, the horizontal line signifies an internal fermion line and the wavy line is a vector meson line.

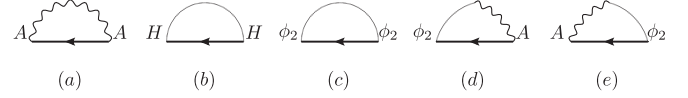


FIG. 1. The fermion self-energy diagrams are shown.

Diagram (a):

This diagram has been discussed thoroughly in Sec. IV. The Feynman amplitude in the BM scheme is denoted by $\Gamma_{1(a)}^{\text{BM}}$:

$$\Gamma_{1(a)}^{\text{BM}} = -ig^2 \int \frac{d^n \ell}{(2\pi)^n} D(A^\mu, A^\nu; \ell) R\gamma^\mu L \frac{1}{\ell + \not{p} - m} R\gamma^\nu L.$$

The corresponding amplitude in the rightmost γ_5 scheme is denoted by $\Gamma_{1(a)}^{\text{R5}}$:

$$\Gamma_{1(a)}^{\text{R5}} = -ig^2 \int \frac{d^n \ell}{(2\pi)^n} D(A^\mu, A^\nu; \ell) \gamma^\mu \frac{\ell + \not{p}}{(\ell + p)^2 - m^2} \gamma^\nu L.$$

The difference has been shown in Sec. IV to be

$$\lim_{n \rightarrow 4} (\Gamma_{1(a)}^{\text{R5}} - \Gamma_{1(a)}^{\text{BM}}) = -\frac{1}{(4\pi)^2} i \frac{g^2}{3} (1 + 2\alpha) \not{p} L.$$

Diagram (b):

There is no γ_5 in the BM amplitude $\Gamma_{1(b)}^{\text{BM}}$. The rightmost γ_5 amplitude $\Gamma_{1(b)}^{\text{R5}}$ is the same as $\Gamma_{1(b)}^{\text{BM}}$ and no finite counterterm is generated:

$$\Gamma_{1(b)}^{\text{R5}} - \Gamma_{1(b)}^{\text{BM}} = 0.$$

Diagram (c):

$$\begin{aligned} \Gamma_{1(c)}^{\text{BM}} &= f^2 \int \frac{d^n \ell}{(2\pi)^n} D(\phi_2, \phi_2, \ell) \gamma_5 \frac{i}{\ell + \not{p} - m} \gamma_5, \\ \Gamma_{1(c)}^{\text{R5}} &= f^2 \int \frac{d^n \ell}{(2\pi)^n} D(\phi_2, \phi_2, \ell) \frac{i}{-\ell - \not{p} - m}, \\ \lim_{n \rightarrow 4} (\Gamma_{1(c)}^{\text{R5}} - \Gamma_{1(c)}^{\text{BM}}) &= if^2 \int \frac{d^n \ell}{(2\pi)^n} D(\phi_2, \phi_2, \ell) \left(\frac{-\ell - \not{p} + m - \gamma_5(\ell + \not{p} + m)\gamma_5}{(\ell + p)^2 - m^2} \right) \\ &= if^2 \int \frac{d^n \ell}{(2\pi)^n} D(\phi_2, \phi_2, \ell) \frac{-2\ell_\Delta}{(\ell + p)^2 - m^2} = 0. \end{aligned}$$

TABLE IV. Counterterms due to diagrams in Fig. 1 are shown in the table.

Figure	$(4\pi)^2 \times (\Gamma^{\text{R5}} - \Gamma^{\text{BM}})$	$(4\pi)^2 \times \text{counterterm}$
1(a)	$-i\frac{g^2}{3}(1+2\alpha)\not{p}L$	$-\frac{g^2}{3}(1+2\alpha)\bar{\psi}Ri\not{p}L\psi$
1(b)	0	0
1(c)	0	0
1(d)	$\frac{i}{2}\alpha(M-\Lambda)fgL$	$\frac{1}{2}\alpha(M-\Lambda)fg\bar{\psi}L\psi$
1(e)	$\frac{i}{2}\alpha(M-\Lambda)fgR$	$\frac{1}{2}\alpha(M-\Lambda)fg\bar{\psi}R\psi$

Diagram (d):

$$\begin{aligned}
 \Gamma_{1(d)}^{\text{BM}} &= (-ig)f \int \frac{d^n \ell}{(2\pi)^n} D(A^\mu, \phi_2; \ell) \gamma_5 \frac{i}{\ell + \not{p} - m} R \gamma^\mu L, \\
 \Gamma_{1(d)}^{\text{R5}} &= (-ig)f \int \frac{d^n \ell}{(2\pi)^n} D(A^\mu, \phi_2; \ell) \frac{i}{-\ell - \not{p} - m} \gamma^\mu L, \\
 \lim_{n \rightarrow 4} (\Gamma_{1(d)}^{\text{R5}} - \Gamma_{1(d)}^{\text{BM}}) &= gf \lim_{n \rightarrow 4} \int \frac{d^n \ell}{(2\pi)^n} D(A^\mu, \phi_2; \ell) \frac{-\ell - \gamma_5 \ell R}{\ell^2 - m^2} \gamma^\mu L \\
 &= \alpha(M - \Lambda) gf \lim_{n \rightarrow 4} \int \frac{d^n \ell}{(2\pi)^n} \frac{-\ell - \gamma_5 \ell R}{(\ell^2 - m^2)^3} \ell L \\
 &= -\alpha(M - \Lambda) gf \lim_{n \rightarrow 4} \int \frac{d^n \ell}{(2\pi)^n} \frac{\ell_\Delta^2}{(\ell^2 - m^2)^3} L = \frac{1}{(4\pi)^2} \frac{i}{2} \alpha(M - \Lambda) fgL.
 \end{aligned}$$

Diagram (e):

$$\begin{aligned}
 \Gamma_{1(e)}^{\text{BM}} &= (-ig)f \int \frac{d^n \ell}{(2\pi)^n} D(\phi_2, A^\mu; \ell) R \gamma^\mu L \frac{i}{\ell + \not{p} - m} \gamma_5, \\
 \Gamma_{1(e)}^{\text{R5}} &= gf \int \frac{d^n \ell}{(2\pi)^n} D(\phi_2, A^\mu; \ell) \gamma^\mu \frac{(\ell + \not{p})R - mL}{(\ell + p)^2 - m^2}, \\
 \lim_{n \rightarrow 4} (\Gamma_{1(e)}^{\text{R5}} - \Gamma_{1(e)}^{\text{BM}}) &= gf \int \frac{d^n \ell}{(2\pi)^n} D(\phi_2, A^\mu; \ell) \frac{\gamma^\mu \ell R - R \gamma^\mu L \ell \gamma_5}{\ell^2 - m^2} \\
 &= -\alpha(M - \Lambda) gf \int \frac{d^n \ell}{(2\pi)^n} \frac{\ell_\Delta^2 R}{(\ell^2 - m^2)^3} \\
 &= \frac{1}{(4\pi)^2} \frac{i}{2} \alpha(M - \Lambda) fgR.
 \end{aligned}$$

To summarize, the amplitudes and finite counterterms due to diagrams in Fig. 1 are tabulated in Table IV.

b. Figure 2: $\bar{\psi}A\psi$ Vertex diagrams

In Fig. 2, $\mu \in \{0, 1, 2, 3\}$ is a polarization the in the first 4 dimensions.

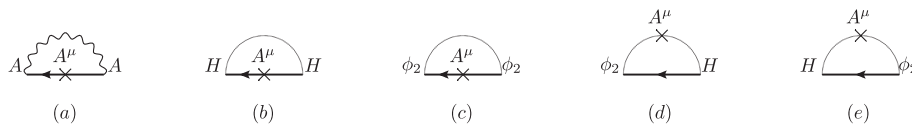


FIG. 2. The diagrams for $\bar{\psi}A\psi$ vertex are shown.

Diagram (a):

$$\begin{aligned}
\Gamma_{2(a)}^{\text{BM}} &= (-ig)^3 \int \frac{d^n \ell}{(2\pi)^n} D(A_\rho, A_\sigma, \ell) R\gamma^\rho L \frac{i}{\ell + \not{p} + \not{k} - m} R\gamma^\mu L \frac{i}{\ell + \not{p} - m} R\gamma^\sigma L, \\
\Gamma_{2(a)}^{\text{R5}} &= -ig^3 \int \frac{d^n \ell}{(2\pi)^n} D(A_\rho, A_\sigma, \ell) \gamma^\rho \frac{\ell + \not{p} + \not{k}}{(\ell + p + k)^2 - m^2} \gamma^\mu \frac{\ell + \not{p}}{(\ell + p)^2 - m^2} \gamma^\sigma L, \\
\Gamma_{2(a)}^{\text{R5}} - \Gamma_{2(a)}^{\text{BM}} &= -ig^3 \int \frac{d^n \ell}{(2\pi)^n} D(A_\rho, A_\sigma, \ell) \frac{\gamma^\rho \ell \gamma^\mu \ell \gamma^\sigma L - R\gamma^\rho L \ell R\gamma^\mu L \ell R\gamma^\sigma L}{(\ell^2 - m^2)^2} \\
&= -g^3 \int \frac{d^n \ell}{(2\pi)^n} \frac{(g^{\rho\sigma} + (\alpha - 1) \frac{\ell^\rho \ell^\sigma}{\ell^2 - m^2})(\gamma^\rho \ell \gamma^\mu \ell \gamma^\sigma - \underline{\gamma^\rho \ell \gamma^\mu \ell \gamma^\sigma})L}{(\ell^2 - m^2)^4} \\
&= -g^3 \int \frac{d^n \ell}{(2\pi)^n} \frac{\frac{(2-n)^2}{n} \ell^2 - \ell^2 + (\alpha - 1) \frac{(\ell^4 - \ell^4)}{\ell^2 - m^2} \gamma^\mu L}{(\ell^2 - m^2)^4} \\
&= \frac{1}{(4\pi)^2} \frac{i}{6} g^3 (7 + 5\alpha) \gamma^\mu L.
\end{aligned}$$

Diagram (b):

$$\begin{aligned}
\Gamma_{2(b)}^{\text{BM}} &= (-ig)(-if)^2 \int \frac{d^n \ell}{(2\pi)^n} D(H, H; \ell) \frac{i}{\ell + \not{p} + \not{k} - m} R\gamma^\mu L \frac{i}{\ell + \not{p} - m}, \\
\Gamma_{2(b)}^{\text{R5}} &= -igf^2 \int \frac{d^n \ell}{(2\pi)^n} D(H, H; \ell) \frac{1}{\ell + \not{p} + \not{k} - m} \gamma^\mu \frac{(\ell + \not{p})R + mL}{(\ell + p)^2 - m^2}, \\
\Gamma_{2(b)}^{\text{R5}} - \Gamma_{2(b)}^{\text{BM}} &= gf^2 \int \frac{d^n \ell}{(2\pi)^n} \frac{1}{\ell^2 - m^2} \frac{1}{\ell - m} \left(\frac{\gamma^\mu \ell R}{\ell^2 - m^2} - \frac{R\gamma^\mu L \ell}{\ell^2 - m^2} \right) \\
&= -gf^2 \int \frac{d^n \ell}{(2\pi)^n} \frac{\ell_\Delta^2 \gamma_5}{(\ell^2 - m^2)^3} = \frac{1}{(4\pi)^2} \frac{1}{2} igf^2 \gamma^\mu \gamma_5.
\end{aligned}$$

Diagram (c):

$$\begin{aligned}
\Gamma_{2(c)}^{\text{BM}} &= -igf^2 \int \frac{d^n \ell}{(2\pi)^n} D(\phi_2; \phi_2; \ell) \gamma_5 \frac{i}{\ell + \not{p} + \not{k} - m} R\gamma^\mu L \frac{i}{\ell + \not{p} - m} \gamma_5 \\
\Gamma_{2(c)}^{\text{R5}} &= -igf^2 \int \frac{d^n \ell}{(2\pi)^n} D(\phi_2; \phi_2; \ell) \frac{1}{\ell + \not{p} + \not{k} + m} \gamma^\mu \frac{(\ell + \not{p})R - mL}{(\ell + p)^2 - m^2} \\
\lim_{n \rightarrow 4} (\Gamma_{2(c)}^{\text{R5}} - \Gamma_{2(c)}^{\text{BM}}) &= gf^2 \int \frac{d^n \ell}{(2\pi)^n} \frac{1}{\ell^2 - m^2} \left(\frac{1}{\ell + m} \gamma^\mu \frac{\ell R}{\ell^2 - m^2} + \gamma_5 \frac{1}{\ell - m} R\gamma^\mu L \frac{1}{\ell - m} \gamma_5 \right) \\
&= -gf^2 \int \frac{d^n \ell}{(2\pi)^n} \frac{\ell_\Delta^2 \gamma_5}{(\ell^2 - m^2)^3} = \frac{1}{(4\pi)^2} i \frac{1}{2} gf^2 \gamma^\mu \gamma_5.
\end{aligned}$$

Diagram (d):

$$\begin{aligned}
\Gamma_{2(d)}^{\text{BM}} &= gf^2 \int \frac{d^n \ell}{(2\pi)^n} D(\phi_2, \phi_2; \ell - k) (2\ell - k)^\mu D(H, H; \ell) \gamma_5 \frac{1}{\ell + \not{p} - m}, \\
\Gamma_{2(d)}^{\text{R5}} &= gf^2 \int \frac{d^n \ell}{(2\pi)^n} D(\phi_2, \phi_2; \ell - k) (2\ell - k)^\mu D(H, H; \ell) \frac{-1}{\ell + \not{p} + m} \gamma_5, \\
\lim_{n \rightarrow 4} (\Gamma_{2(d)}^{\text{R5}} - \Gamma_{2(d)}^{\text{BM}}) &= gf^2 \int \frac{d^n \ell}{(2\pi)^n} D(\phi_2, \phi_2; \ell) D(H, H; \ell) 2\ell^\mu \left(\frac{-1}{\ell + m} \gamma_5 - \gamma_5 \frac{1}{\ell - m} \right) \\
&= -4gf^2 \int \frac{d^n \ell}{(2\pi)^n} D(\phi_2, \phi_2; \ell) D(H, H; \ell) \frac{\ell^\mu \ell_\Delta \gamma_5}{(\ell^2 - m^2)} = 0.
\end{aligned}$$

TABLE V. Counterterms due to diagrams in Fig. 2 are shown in the table.

Figure	$(4\pi)^2 \times (\Gamma^{\text{R5}} - \Gamma^{\text{BM}})$	$(4\pi)^2 \times \text{counterterm}$
2(a)	$\frac{i}{6} g^3 (7 + 5\alpha) \gamma^\mu L$	$\frac{1}{6} g^3 (7 + 5\alpha) \bar{\psi} R A L \psi$
2(b)	$\frac{1}{2} i g f^2 \gamma^\mu \gamma_5$	$\frac{1}{2} g f^2 \bar{\psi} A \gamma_5 \psi$
2(c)	$\frac{1}{2} i g f^2 \gamma^\mu \gamma_5$	$\frac{1}{2} g f^2 \bar{\psi} A \gamma_5 \psi$
2(e)	0	0
2(e)	0	0

Diagram (e):

$$\Gamma_{2(e)}^{\text{BM}} = g f^2 \int \frac{d^n \ell}{(2\pi)^n} D(H, H; \ell - k) (k - 2\ell)^\mu D(\phi_2, \phi_2; \ell) \frac{1}{\ell + \not{p} - m} \gamma_5,$$

$$\Gamma_{2(e)}^{\text{R5}} = g f^2 \int \frac{d^n \ell}{(2\pi)^n} D(H, H; \ell - k) (k - 2\ell)^\mu D(\phi_2, \phi_2; \ell) \frac{1}{\ell + \not{p} - m} \gamma_5,$$

$$\Gamma_{2(e)}^{\text{R5}} - \Gamma_{2(e)}^{\text{BM}} = 0.$$

To summarize, the amplitudes and finite counterterms due to diagrams in Fig. 2 are tabulated in Table V.

c. Figure 3: $\bar{\psi} H \psi$ Vertex diagrams

Diagram (a):

$$\Gamma_{3(a)}^{\text{BM}} = -i f g^2 \int \frac{d^n \ell}{(2\pi)^n} D(A_\mu, A_\nu; \ell) R \gamma^\mu L \frac{1}{\ell + \not{p} + \not{k} - m} \frac{1}{\ell + \not{p} - m} R \gamma^\nu L,$$

$$\Gamma_{3(a)}^{\text{R5}} = -i f g^2 \int \frac{d^n \ell}{(2\pi)^n} D(A_\mu, A_\nu; \ell) \gamma^\mu \frac{m(2\ell + 2\not{p} + \not{k})}{((\ell + \not{p} + \not{k})^2 - m^2)((\ell + \not{p})^2 - m^2)} \gamma^\nu L,$$

$$\lim_{n \rightarrow 4} (\Gamma_{3(a)}^{\text{R5}} - \Gamma_{3(a)}^{\text{BM}}) = 2f g^2 \int \frac{d^n \ell}{(2\pi)^n} \frac{g_{\mu\nu} + (\alpha - 1) \frac{\ell_\mu \ell_\nu}{\ell^2}}{(\ell^2 - m^2)^3} \left(\begin{array}{c} m \gamma^\mu \ell \gamma^\nu \\ -\underline{\gamma}^\mu (m + \ell_\Delta) \underline{\ell} \gamma^\nu \end{array} \right) L$$

$$= -2f g^2 \int \frac{d^n \ell}{(2\pi)^n} \frac{g_{\mu\nu} + (\alpha - 1) \frac{\ell_\mu \ell_\nu}{\ell^2}}{(\ell^2 - m^2)^3} \underline{\gamma}^\mu \ell_\Delta \underline{\ell} \gamma^\nu L = 0.$$

Diagram (b):

No γ_5 is involved, and therefore

$$\Gamma_{3(b)}^{\text{R5}} - \Gamma_{3(b)}^{\text{BM}} = 0.$$

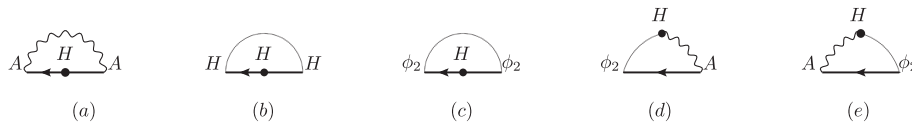


FIG. 3. The diagrams for $\bar{\psi} H \psi$ vertex are shown.

Diagram (c):

$$\begin{aligned}\Gamma_{3(c)}^{\text{BM}} &= -if^3 \int \frac{d^n \ell}{(2\pi)^n} D(\phi_2, \phi_2; \ell) \gamma_5 \frac{1}{\ell + \not{p} + \not{k} - m} \frac{1}{\ell + \not{p} - m} \gamma_5, \\ \Gamma_{3(c)}^{\text{R5}} &= -if^3 \int \frac{d^n \ell}{(2\pi)^n} D(\phi_2, \phi_2; \ell) \frac{1}{\ell + \not{p} + \not{k} + m} \frac{1}{\ell + \not{p} + m}, \\ \lim_{n \rightarrow 4} (\Gamma_{3(c)}^{\text{R5}} - \Gamma_{3(c)}^{\text{BM}}) &= f^3 \int \frac{d^n \ell}{(2\pi)^n} \frac{1}{(\ell^2 - m^2)} \left(\left(\frac{1}{\ell + m} \right)^2 - \gamma_5 \left(\frac{1}{\ell - m} \right)^2 \gamma_5 \right) \\ &= f^3 \int \frac{d^n \ell}{(2\pi)^n} \frac{1}{(\ell^2 - m^2)^3} (\ell^2 - \gamma_5 \ell^2 \gamma_5) = 0.\end{aligned}$$

Diagram (d):

$$\begin{aligned}\Gamma_{3(d)}^{\text{BM}} &= g^2 f \int \frac{d^n \ell}{(2\pi)^n} D(\phi_2, \phi_2; \ell) D(A_\mu, A_\nu; \ell + k) (\ell - k)^\mu \gamma_5 \frac{1}{\ell + \not{p} + \not{k} - m} R \gamma^\nu L, \\ \Gamma_{3(d)}^{\text{R5}} &= -g^2 f \int \frac{d^n \ell}{(2\pi)^n} D(\phi_2, \phi_2; \ell) D(A_\mu, A_\nu; \ell + k) (\ell - k)^\mu \frac{1}{\ell + \not{p} + \not{k} + m} \gamma^\nu L, \\ \lim_{n \rightarrow 4} (\Gamma_{3(d)}^{\text{R5}} - \Gamma_{3(d)}^{\text{BM}}) &= -g^2 f \int \frac{d^n \ell}{(2\pi)^n} D(\phi_2, \phi_2; \ell) D(A_\mu, A_\nu; \ell) \ell^\mu \left(\frac{1}{\ell + m} \gamma^\nu L + \gamma_5 \frac{1}{\ell - m} R \gamma^\nu L \right) \\ &= -g^2 f \int \frac{d^n \ell}{(2\pi)^n} \frac{\alpha}{(\ell^2 - m^2)^3} (\ell^2 L + \gamma_5 \ell R \ell L) \\ &= -g^2 f \int \frac{d^n \ell}{(2\pi)^n} \frac{\alpha \ell_\Delta^2}{(\ell^2 - m^2)^3} L \\ &= \frac{1}{(4\pi)^2} i \frac{\alpha g^2 f}{2} L.\end{aligned}$$

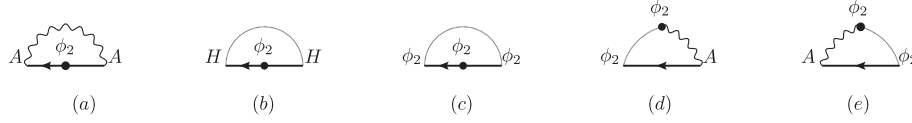
Diagram (e):

$$\begin{aligned}\Gamma_{3(e)}^{\text{BM}} &= gf \int \frac{d^n \ell}{(2\pi)^n} D(A_\mu, A_\nu; \ell) (-g(\ell + 2k)^\mu) D(\phi_2, \phi_2; \ell + k) R \gamma^\nu L \frac{1}{\ell + \not{p} + \not{k} - m} \gamma_5, \\ \Gamma_{3(e)}^{\text{R5}} &= gf \int \frac{d^n \ell}{(2\pi)^n} D(A_\mu, A_\nu; \ell) (-g(\ell + 2k)^\mu) D(\phi_2, \phi_2; \ell + k) \gamma^\nu \frac{(\ell + \not{p} + \not{k})R - mL}{(\ell + \not{p} + \not{k})^2 - m^2}, \\ \lim_{n \rightarrow 4} (\Gamma_{3(e)}^{\text{R5}} - \Gamma_{3(e)}^{\text{BM}}) &= -g^2 f \int \frac{d^n \ell}{(2\pi)^n} \frac{\alpha \ell_\Delta^2}{(\ell^2 - m^2)^3} (\ell^2 R - R \ell L \ell \gamma_5) \\ &= -g^2 f \int \frac{d^n \ell}{(2\pi)^n} \frac{\alpha \ell_\Delta^2}{(\ell^2 - m^2)^3} R \\ &= \frac{1}{(4\pi)^2} i \frac{\alpha g^2 f}{2} R.\end{aligned}$$

To summarize, the amplitudes and finite counterterms due to diagrams in Fig. 3 are tabulated in Table VI.

TABLE VI. Counterterms due to diagrams in Fig. 3 are shown in the table.

Figure	$(4\pi)^2 \times (\Gamma^{\text{R5}} - \Gamma^{\text{BM}})$	$(4\pi)^2 \times \text{counterterm}$
3(a)	0	0
3(b)	0	0
3(c)	0	0
3(d)	$i \frac{\alpha g^2 f}{2} L$	$\frac{\alpha g^2 f}{2} \bar{\psi} H L \psi$
3(e)	$i \frac{\alpha g^2 f}{2} R$	$\frac{\alpha g^2 f}{2} \bar{\psi} H R \psi$


 FIG. 4. The diagrams for $\bar{\psi}\phi_2\psi$ vertex are shown.

d. Figure 4: $\bar{\psi}\phi_2\psi$ Vertex diagrams

Diagram (a):

$$\begin{aligned}\Gamma_{4(a)}^{\text{BM}} &= fg^2 \int \frac{d^n \ell}{(2\pi)^n} D(A_\mu, A_\nu; \ell) R\gamma^\mu L \frac{1}{\ell + \not{p} + \not{k} - m} \gamma_5 \frac{1}{\ell + \not{p} - m} R\gamma^\nu L, \\ \Gamma_{4(a)}^{\text{R5}} &= fg^2 \int \frac{d^n \ell}{(2\pi)^n} D(A_\mu, A_\nu; \ell) \gamma^\mu \frac{m \not{k}}{((\ell + p + k)^2 - m^2)((\ell + p)^2 - m^2)} \gamma^\nu L, \\ \lim_{n \rightarrow 4} (\Gamma_{4(a)}^{\text{R5}} - \Gamma_{4(a)}^{\text{BM}}) &= -ifg^2 \int \frac{d^n \ell}{(2\pi)^n} \frac{g_{\mu\nu} + (\alpha - 1) \frac{\ell_\mu \ell_\nu}{\ell^2}}{(\ell^2 - m^2)^3} (-2m \underline{\gamma}^\mu \ell_\Delta \underline{\gamma}^\nu) L = 0.\end{aligned}$$

Diagram (b):

$$\begin{aligned}\Gamma_{4(b)}^{\text{BM}} &= f^3 \int \frac{d^n \ell}{(2\pi)^n} D(\phi_2, \phi_2; \ell) \frac{1}{\ell + \not{p} + \not{k} - m} \gamma_5 \frac{1}{\ell + \not{p} - m}, \\ \Gamma_{4(b)}^{\text{R5}} &= -f^3 \int \frac{d^n \ell}{(2\pi)^n} D(\phi_2, \phi_2; \ell) \frac{1}{\ell + \not{p} + \not{k} - m} \frac{1}{\ell + \not{p} + m} \gamma_5, \\ \lim_{n \rightarrow 4} (\Gamma_{4(b)}^{\text{R5}} - \Gamma_{4(b)}^{\text{BM}}) &= -if^3 \int \frac{d^n \ell}{(2\pi)^n} \frac{1}{(\ell^2 - m^2)^2} \left(\frac{1}{(\ell^2 - m^2)} \gamma_5 + \frac{1}{\ell - m} \gamma_5 \frac{1}{\ell - m} \right) \\ &= -if^3 \int \frac{d^n \ell}{(2\pi)^n} \frac{1}{(\ell^2 - m^2)^2} \left(\gamma_5 + \frac{1}{(\ell^2 - m^2)} \ell \gamma_5 \ell \right) \\ &= -2if^3 \int \frac{d^n \ell}{(2\pi)^n} \frac{\ell_\Delta^2}{(\ell^2 - m^2)^3} \gamma_5 \\ &= -\frac{1}{(4\pi)^2} f^3 \gamma_5.\end{aligned}$$

Diagram (c)

$$\begin{aligned}\Gamma_{4(c)}^{\text{BM}} &= -f^3 \int \frac{d^n \ell}{(2\pi)^n} D(\phi_2, \phi_2; \ell) \gamma_5 \frac{1}{\ell + \not{p} + \not{k} - m} \gamma_5 \frac{1}{\ell + \not{p} - m} \gamma_5, \\ \Gamma_{4(c)}^{\text{R5}} &= f^3 \int \frac{d^n \ell}{(2\pi)^n} D(\phi_2, \phi_2; \ell) \frac{1}{\ell + \not{p} + \not{k} + m} \frac{1}{\ell + \not{p} - m} \gamma_5, \\ \lim_{n \rightarrow 4} (\Gamma_{4(c)}^{\text{R5}} - \Gamma_{4(c)}^{\text{BM}}) &= if^3 \int \frac{d^n \ell}{(2\pi)^n} \frac{1}{(\ell^2 - m^2)^2} \left(\gamma_5 + \frac{1}{(\ell^2 - m^2)} \gamma_5 \ell \gamma_5 \ell \gamma_5 \right) \\ &= 2if^3 \int \frac{d^n \ell}{(2\pi)^n} \frac{\ell_\Delta^2}{(\ell^2 - m^2)^3} \gamma_5 \\ &= \frac{1}{(4\pi)^2} f^3 \gamma_5.\end{aligned}$$

TABLE VII. Counterterms due to diagrams in Fig. 4 are shown in the table.

Figure	$(4\pi)^2 \times (\Gamma^{R5} - \Gamma^{BM})$	$(4\pi)^2 \times \text{counterterm}$
4(a)	0	0
4(b)	$-f^3 \gamma_5$	$if^3 \bar{\psi} \phi_2 \gamma_5 \psi$
4(c)	$f^3 \gamma_5$	$-if^3 \bar{\psi} \phi_2 \gamma_5 \psi$
4(d)	$\frac{\alpha g^2 f}{2} L$	$-i \frac{\alpha g^2 f}{2} \bar{\psi} \phi_2 L \psi$
4(e)	$-\frac{\alpha g^2 f}{2} R$	$i \frac{\alpha g^2 f}{2} \bar{\psi} \phi_2 R \psi$

Diagram (d):

$$\begin{aligned} \Gamma_{4(d)}^{BM} &= -ifg^2 \int \frac{d^n \ell}{(2\pi)^n} D(H, H; \ell) (k - \ell)^\mu D(A_\mu, A_\nu; \ell + k) \frac{1}{\ell + \not{p} + k - m} R \gamma^\nu L, \\ \Gamma_{4(d)}^{R5} &= -ifg^2 \int \frac{d^n \ell}{(2\pi)^n} D(H, H; \ell) (k - \ell)^\mu D(A_\mu, A_\nu; \ell + k) \frac{1}{\ell + \not{p} + k - m} \gamma^\nu L, \\ \lim_{n \rightarrow 4} (\Gamma_{4(d)}^{R5} - \Gamma_{4(d)}^{BM}) &= -ifg \int \frac{d^n \ell}{(2\pi)^n} D(H, H; \ell) g (k - \ell)^\mu D(A_\mu, A_\nu; \ell + k) \frac{1}{\ell - m} (\gamma^\nu L - R \gamma^\nu L) \\ &= ifg^2 \int \frac{d^n \ell}{(2\pi)^n} \frac{\alpha \ell_\Delta^2}{(\ell^2 - m^2)^3} L = \frac{1}{(4\pi)^2} \frac{1}{2} \alpha f g^2 L. \end{aligned}$$

Diagram (e):

$$\begin{aligned} \Gamma_{4(e)}^{BM} &= -igf \int \frac{d^n \ell}{(2\pi)^n} D(A_\mu, A_\nu; \ell) g (\ell + 2k)^\nu D(H, H; \ell + k) R \gamma^\mu L \frac{1}{\ell + \not{p} + k - m}, \\ \Gamma_{4(e)}^{R5} &= -igf \int \frac{d^n \ell}{(2\pi)^n} D(A_\mu, A_\nu; \ell) g (\ell + 2k)^\nu D(H, H; \ell + k) \gamma^\mu \frac{(\ell + \not{p} + k) R + mL}{(\ell + p + k)^2 - m^2}, \\ \lim_{n \rightarrow 4} (\Gamma_{4(e)}^{R5} - \Gamma_{4(e)}^{BM}) &= -igf \int \frac{d^n \ell}{(2\pi)^n} D(A_\mu, A_\nu; \ell) g \ell^\nu D(H, H; \ell) \left(\gamma^\mu \frac{\ell R}{\ell^2 - m^2} - R \gamma^\mu L \frac{1}{\ell - m} \right) \\ &= -ig^2 f \int \frac{d^n \ell}{(2\pi)^n} \frac{\alpha \ell_\Delta^2}{(\ell^2 - m^2)^3} R = -\frac{1}{(4\pi)^2} \frac{\alpha g^2 f}{2} R. \end{aligned}$$

To summarize, the amplitudes and finite counterterms due to diagrams in Fig. 4 are tabulated in Table VII.

e. Figure 5: One-fermion-loop 2-point 1PI

Diagram (a):

No γ_5 occurs in the amplitude. Thus,

$$\Gamma_{5(a)}^{R5} - \Gamma_{5(a)}^{BM} = 0.$$

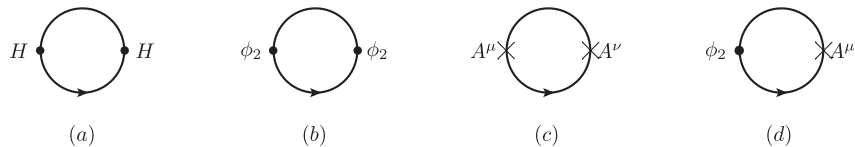


FIG. 5. The diagrams for 2-point 1PI are shown.

Diagram (b):

$$\begin{aligned}
 \Gamma_{5(b)}^{\text{BM}} &= -f^2 \text{tr} \int \frac{d^n \ell}{(2\pi)^n} \frac{i}{\ell - m} \gamma_5 \frac{i}{\ell - \not{p} - m}, \\
 \Gamma_{5(b)}^{\text{R5}} &= f^2 \text{tr} \int \frac{d^n \ell}{(2\pi)^n} \frac{i}{\ell - m} \frac{i}{\ell - \not{p} + m}, \\
 \lim_{n \rightarrow 4} (\Gamma_{5(b)}^{\text{R5}} - \Gamma_{5(b)}^{\text{BM}}) &= -f^2 \text{tr} \int \frac{d^n \ell}{(2\pi)^n} \frac{1}{\ell - m} \left(\frac{1}{\ell - \not{p} + m} + \gamma_5 \frac{1}{\ell - \not{p} - m} \gamma_5 \right) \\
 &= -f^2 \int \frac{d^n \ell}{(2\pi)^n} \frac{\text{tr}[(\ell + m)2\ell_\Delta]}{(\ell^2 - m^2)((\ell - p)^2 - m^2)} \\
 &= -8f^2 \int \frac{d^n \ell}{(2\pi)^n} \ell_\Delta^2 \left(\frac{1}{(\ell^2 - m^2)^2} + \frac{2\ell \cdot p - p^2}{(\ell^2 - m^2)^3} + \frac{(2\ell \cdot p - p^2)^2}{(\ell^2 - m^2)^4} \right) \\
 &= \frac{1}{(4\pi)^2} i f^2 \left(8m^2 - \frac{4}{3} p^2 \right).
 \end{aligned}$$

Diagram (c):

$$\begin{aligned}
 \Gamma_{5(c)}^{\text{BM}} &= -g^2 \text{tr} \int \frac{d^n \ell}{(2\pi)^n} \frac{1}{\ell - m} R \gamma^\mu L \frac{1}{\ell - \not{p} - m} R \gamma^\nu L, \\
 \Gamma_{5(c)}^{\text{R5}} &= -g^2 \text{tr} \int \frac{d^n \ell}{(2\pi)^n} \frac{1}{\ell - m} \gamma^\mu \frac{\ell - \not{p}}{(\ell - p)^2 - m^2} \gamma^\nu L, \\
 \lim_{n \rightarrow 4} (\Gamma_{5(c)}^{\text{R5}} - \Gamma_{5(c)}^{\text{BM}}) &= -g^2 \text{tr} \int \frac{d^n \ell}{(2\pi)^n} \frac{1}{\ell - m} \gamma^\mu \left(\frac{\ell - L \ell R}{(\ell - p)^2 - m^2} \right) \gamma^\nu L \\
 &= 2g^{\mu\nu} g^2 \int \frac{d^n \ell}{(2\pi)^n} \ell_\Delta^2 \left(\frac{1}{(\ell^2 - m^2)^2} + \frac{2\ell \cdot p - p^2}{(\ell^2 - m^2)^3} + \frac{(2\ell \cdot p - p^2)^2}{(\ell^2 - m^2)^4} \right) \\
 &= \frac{1}{(4\pi)^2} i g^{\mu\nu} g^2 \left(-2m^2 + \frac{1}{3} p^2 \right). \tag{A1}
 \end{aligned}$$

Diagram (d):

$$\begin{aligned}
 \Gamma_{5(d)}^{\text{BM}} &= -i f g \int \frac{d^n \ell}{(2\pi)^n} \text{tr} \left(\frac{1}{\ell - \not{p} - m} \gamma_5 \frac{1}{\ell - m} R \gamma^\mu L \right), \\
 \Gamma_{5(d)}^{\text{R5}} &= -i f g \int \frac{d^n \ell}{(2\pi)^n} \text{tr} \left(\frac{1}{\ell - \not{p} - m} \frac{1}{-\ell - m} \gamma^\mu L \right), \\
 \lim_{n \rightarrow 4} (\Gamma_{5(d)}^{\text{R5}} - \Gamma_{5(d)}^{\text{BM}}) &= i f g \int \frac{d^n \ell}{(2\pi)^n} \text{tr} \left(\frac{1}{\ell - \not{p} - m} \left(\frac{1}{\ell + m} + \gamma_5 \frac{1}{\ell - m} R \right) \gamma^\mu L \right) \\
 &= i f g \int \frac{d^n \ell}{(2\pi)^n} \text{tr} \left(\frac{2(\ell - \not{p} + m) \ell_\Delta \gamma^\mu L}{((\ell - p)^2 - m^2)(\ell^2 - m^2)} \right) = 0.
 \end{aligned}$$

To summarize, the amplitudes and finite counterterms due to diagrams in Fig. 5 are tabulated in Table VIII.

TABLE VIII. Counterterms due to diagrams in Fig. 5 are shown in the table.

Figure	$(4\pi)^2 \times (\Gamma^{\text{R5}} - \Gamma^{\text{BM}})$	$(4\pi)^2 \times \text{counterterm}$
5(a)	0	0
5(b)	$i f^2 (8m^2 - \frac{4}{3} p^2)$	$4m^2 f^2 (\phi_2)^2 - \frac{2}{3} f^2 (\partial_\mu \phi_2) (\partial^\mu \phi_2)$
5(c)	$i g^{\mu\nu} g^2 (-2m^2 + \frac{1}{3} p^2)$	$-g^2 m^2 A^2 + \frac{1}{6} g^2 (\partial_\mu A_\nu) (\partial^\mu A^\nu)$
5(d)	0	0

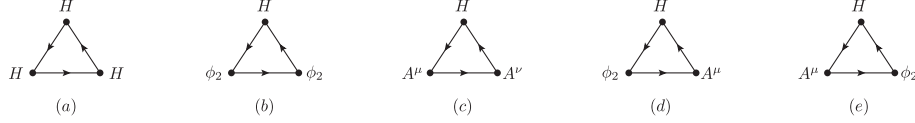


FIG. 6. The diagrams for 3-point 1PI are shown.

f. Figure 6: One-fermion-loop 3-point 1PI

Diagram (a):

No γ_5 is involved and therefore there is no finite counterterm.

Diagram (b):

$$\begin{aligned}\Gamma_{6(b)}^{\text{BM}} &= f^3 \text{tr} \int \frac{d^n \ell}{(2\pi)^n} \frac{1}{\ell - m} \frac{1}{\ell - \not{p}_1 - m} \gamma_5 \frac{1}{\ell - \not{p}_1 - \not{p}_2 - m} \gamma_5, \\ \Gamma_{6(b)}^{\text{R5}} &= -f^3 \text{tr} \int \frac{d^n \ell}{(2\pi)^n} \frac{1}{\ell - m} \frac{1}{\ell - \not{p}_1 - m} \frac{1}{\ell - \not{p}_1 - \not{p}_2 + m}, \\ \lim_{n \rightarrow 4} (\Gamma_{6(b)}^{\text{R5}} - \Gamma_{6(b)}^{\text{BM}}) &= f^3 \text{tr} \int \frac{d^n \ell}{(2\pi)^n} \frac{1}{\ell - m} \frac{1}{\ell - \not{p}_1 - m} \frac{(-\ell + \not{p}_1 + \not{p}_2 + m) - \gamma_5(\ell - \not{p}_1 - \not{p}_2 + m)\gamma_5}{(\ell - \not{p}_1 - \not{p}_2)^2 - m^2} \\ &= -2f^3 \text{tr} \int \frac{d^n \ell}{(2\pi)^n} \frac{(\ell + m)(\ell - \not{p}_1 + m)\ell_\Delta}{(\ell^2 - m^2)((\ell - p_1)^2 - m^2)((\ell - p_1 - p_2)^2 - m^2)} \\ &= -2f^3 \text{tr} \int \frac{d^n \ell}{(2\pi)^n} \frac{(\not{p}_1 + 2m)\ell_\Delta^2}{(\ell^2 - m^2)^3} = \frac{1}{(4\pi)^2} 8if^3 m.\end{aligned}$$

There is another diagram corresponding to the exchange of the two ϕ_2 fields or the reverse of the fermion-loop direction which also yields the same amplitude $\frac{1}{(4\pi)^2} 8if^3 m$.

Diagram (c):

$$\begin{aligned}\Gamma_{6(c)}^{\text{BM}} &= -fg^2 \text{tr} \int \frac{d^n \ell}{(2\pi)^n} \frac{1}{\ell - m} \frac{1}{\ell - \not{p}_1 - m} R\gamma^\mu \frac{1}{\ell - \not{p}_1 - \not{p}_2 - m} R\gamma^\nu L, \\ \Gamma_{6(c)}^{\text{R5}} &= -fg^2 \text{tr} \int \frac{d^n \ell}{(2\pi)^n} \frac{1}{\ell - m} \frac{1}{\ell - \not{p}_1 - m} \gamma^\mu \frac{\ell - \not{p}_1 - \not{p}_2}{(\ell - \not{p}_1 - \not{p}_2)^2 - m^2} \gamma^\nu L, \\ \lim_{n \rightarrow 4} (\Gamma_{6(c)}^{\text{R5}} - \Gamma_{6(c)}^{\text{BM}}) &= -fg^2 \int \frac{d^n \ell}{(2\pi)^n} \frac{\text{tr}[(\ell + m)(\ell - \not{p}_1 + m)\gamma^\mu \ell_\Delta \gamma^\nu L]}{(\ell^2 - m^2)((\ell - p_1)^2 - m^2)((\ell - p_1 - p_2)^2 - m^2)} \\ &= 4fg^2 \int \frac{d^n \ell}{(2\pi)^n} \frac{\ell_\Delta^2 mg^{\mu\nu}}{(\ell^2 - m^2)^3} \\ &= -\frac{1}{(4\pi)^2} 2ifg^2 mg^{\mu\nu}.\end{aligned}$$

Interchanging the two external A fields gives us another topologically different diagram whose amplitude is also equal to $-\frac{1}{(4\pi)^2} 2ig^2 fmg^{\mu\nu}$.

Diagram (d):

$$\begin{aligned}\Gamma_{6(d)}^{\text{BM}} &= -if^2 g \text{tr} \int \frac{d^n \ell}{(2\pi)^n} \frac{1}{\ell - m} \frac{1}{\ell - \not{p}_1 - m} \gamma_5 \frac{1}{\ell - \not{p}_1 - \not{p}_2 - m} R\gamma^\nu L, \\ \Gamma_{6(d)}^{\text{R5}} &= if^2 g \text{tr} \int \frac{d^n \ell}{(2\pi)^n} \frac{1}{\ell - m} \frac{1}{\ell - \not{p}_1 - m} \frac{1}{\ell - \not{p}_1 - \not{p}_2 - m} R\gamma^\nu L, \\ \lim_{n \rightarrow 4} (\Gamma_{6(d)}^{\text{R5}} - \Gamma_{6(d)}^{\text{BM}}) &= if^2 g \int \frac{d^n \ell}{(2\pi)^n} \frac{2 \text{tr}[(\ell + m)(\ell - \not{p}_1 + m)\ell_\Delta \gamma^\nu L]}{(\ell^2 - m^2)((\ell - p_1)^2 - m^2)((\ell - p_1 - p_2)^2 - m^2)} \\ &= if^2 g \int \frac{d^n \ell}{(2\pi)^n} \frac{\ell_\Delta^2}{(\ell^2 - m^2)^3} \text{tr}[\not{p}_1 \gamma^\nu] \\ &= \frac{1}{(4\pi)^2} 2f^2 g p_1^\nu.\end{aligned}$$

TABLE IX. Counterterms due to diagrams in Fig. 6 are shown in the table.

Figure	$(4\pi)^2 \times$ $(\Gamma^{\text{R5}} - \Gamma^{\text{BM}})$	Multiplicity	$(4\pi)^2 \times$ counterterm
6(a)	0	2	0
6(b)	$8if^3m$	2	$8f^3mH(\phi_2)^2$
6(c)	$-2ifg^2mg^{\mu\nu}$	2	$-2fg^2mHA^2$
6(d)	$2f^2gp_1^\nu$	1	$2f^2g\phi_2(\partial_\mu H)A^\mu$
6(e)	$2f^2gp_1^\nu$	1	$2f^2g\phi_2(\partial_\mu H)A^\mu$

Diagram (e):

$$\begin{aligned}
 \Gamma_{6(e)}^{\text{BM}} &= -if^2g \text{tr} \int \frac{d^n \ell}{(2\pi)^n} \frac{1}{\ell - m} \frac{1}{\ell - p_1 - m} R\gamma^\nu L \frac{1}{\ell - p_1 - p_2 - m} \gamma_5, \\
 \Gamma_{6(e)}^{\text{R5}} &= -if^2g \text{tr} \int \frac{d^n \ell}{(2\pi)^n} \frac{1}{\ell - m} \frac{1}{\ell - p_1 - m} \gamma^\nu \frac{(\ell - p_1 - p_2)R - mL}{((\ell - p_1 - p_2)^2 - m^2)}, \\
 \lim_{n \rightarrow 4} (\Gamma_{6(e)}^{\text{R5}} - \Gamma_{6(e)}^{\text{BM}}) &= -if^2g \int \frac{d^n \ell}{(2\pi)^n} \frac{\text{tr}[(\ell + m)(\ell - p_1 + m)\gamma^\nu \ell_\Delta]}{(\ell^2 - m^2)((\ell - p_1)^2 - m^2)((\ell - p_1 - p_2)^2 - m^2)} \\
 &= if^2g \int \frac{d^n \ell}{(2\pi)^n} \frac{\ell_\Delta^2}{(\ell^2 - m^2)^3} \text{tr}[p_1 \gamma^\nu] \\
 &= \frac{1}{(4\pi)^2} 2f^2gp_1^\nu.
 \end{aligned}$$

To summarize, the amplitudes and finite counterterms due to diagrams in Fig. 6 are tabulated in Table IX. Note the column ‘‘Multiplicity’’ indicates the combinatorial factor that needs to be multiplied.

g. Figure 7: One-fermion-loop 4-point 1PI

Only T_0 order terms may be divergent. For the sake of simplicity, we may assume all the external momenta are zero.

Diagram (a):

No γ_5 is involved and therefore diagram (a) generates no finite counterterm.

Diagram (b):

$$\begin{aligned}
 \Gamma_{7(b)}^{\text{BM}} &= f^4 \text{tr} \int \frac{d^n \ell}{(2\pi)^n} \frac{1}{\ell - m} \frac{1}{\ell - m} \frac{1}{\ell - m} \gamma_5 \frac{1}{\ell - m} \gamma_5, \\
 \Gamma_{7(b)}^{\text{R5}} &= f^4 \text{tr} \int \frac{d^n \ell}{(2\pi)^n} \frac{1}{\ell - m} \frac{1}{\ell - m} \frac{1}{\ell - m} \frac{-1}{\ell + m}, \\
 \lim_{n \rightarrow 4} (\Gamma_{7(b)}^{\text{R5}} - \Gamma_{7(b)}^{\text{BM}}) &= f^4 \lim_{n \rightarrow 4} \text{tr} \int \frac{d^n \ell}{(2\pi)^n} \frac{\ell \ell \ell}{(\ell^2 - m^2)^4} (-\ell - \gamma_5 \ell \gamma_5) \\
 &= -2f^4 \lim_{n \rightarrow 4} \int \frac{d^n \ell}{(2\pi)^n} \frac{\text{tr}[\ell^2 \ell_\Delta^2]}{(\ell^2 - m^2)^4} = \frac{1}{(4\pi)^2} 4if^4.
 \end{aligned}$$

Exchanging the two H and the two ϕ_2 gives a combinatorial factor of 4. The total counterterm amplitude is $\frac{1}{(4\pi)^2} 4 \times 4if^4 = \frac{1}{(4\pi)^2} 16if^4$.

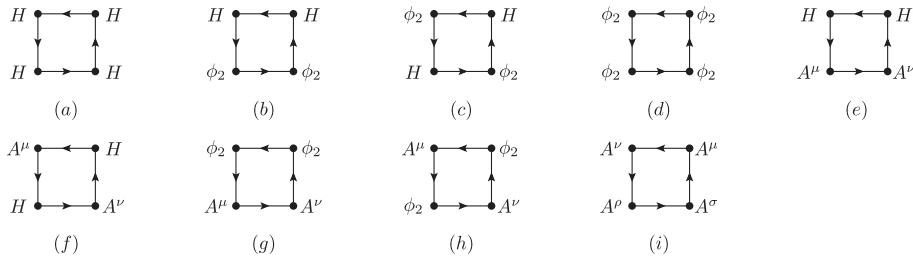


FIG. 7. The diagrams for 4-point 1PI are shown.

Diagram (c):

$$\begin{aligned}\Gamma_{7(c)}^{\text{BM}} &= f^4 \text{tr} \int \frac{d^n \ell}{(2\pi)^n} \frac{1}{\ell - m} \frac{1}{\ell - m} \gamma_5 \frac{1}{\ell - m} \frac{1}{\ell - m} \gamma_5, \\ \Gamma_{7(c)}^{\text{R5}} &= f^4 \text{tr} \int \frac{d^n \ell}{(2\pi)^n} \frac{1}{\ell - m} \frac{1}{\ell - m} \frac{1}{\ell + m} \frac{1}{\ell + m}, \\ \lim_{n \rightarrow 4} (\Gamma_{7(c)}^{\text{R5}} - \Gamma_{7(c)}^{\text{BM}}) &= f^4 \text{tr} \int \frac{d^n \ell}{(2\pi)^n} \frac{\ell \ell \ell \ell - \ell \ell \gamma_5 \ell \ell \gamma_5}{(\ell^2 - m^2)^4} = 0.\end{aligned}$$

Diagram (d):

$$\begin{aligned}\Gamma_{7(d)}^{\text{BM}} &= -f^4 \text{tr} \int \frac{d^n \ell}{(2\pi)^n} \frac{1}{\ell - m} \gamma_5 \frac{1}{\ell - m} \gamma_5 \frac{1}{\ell - m} \gamma_5 \frac{1}{\ell - m} \gamma_5, \\ \Gamma_{7(d)}^{\text{R5}} &= -f^4 \text{tr} \int \frac{d^n \ell}{(2\pi)^n} \frac{1}{\ell - m} \frac{1}{\ell + m} \frac{1}{\ell - m} \frac{1}{\ell + m}, \\ \lim_{n \rightarrow 4} (\Gamma_{7(d)}^{\text{R5}} - \Gamma_{7(d)}^{\text{BM}}) &= -f^4 \int \frac{d^n \ell}{(2\pi)^n} \frac{\text{tr}[\ell^4 - \ell \gamma_5 \ell \gamma_5 \ell \gamma_5 \ell \gamma_5]}{(\ell^2 - m^2)^4} \\ &= -32f^4 \int \frac{d^n \ell}{(2\pi)^n} \frac{\ell_\Delta^2 \ell^2}{(\ell^2 - m^2)^4} = \frac{1}{(4\pi)^2} \frac{32}{3} if^4.\end{aligned}$$

Permutation of the four ϕ_2 on a loop gives a combinatorial factor of 3!. The total counterterm amplitude due to this type of diagram is $3! \times \frac{1}{(4\pi)^2} \frac{32}{3} if^4 = \frac{1}{(4\pi)^2} 64if^4$.

Diagram (e):

$$\begin{aligned}\Gamma_{7(e)}^{\text{BM}} &= -f^2 g^2 \text{tr} \int \frac{d^n \ell}{(2\pi)^n} \frac{1}{\ell - m} \frac{1}{\ell - m} \frac{1}{\ell - m} R\gamma^\mu L \frac{1}{\ell - m} R\gamma^\nu L, \\ \Gamma_{7(e)}^{\text{R5}} &= -f^2 g^2 \text{tr} \int \frac{d^n \ell}{(2\pi)^n} \frac{1}{\ell - m} \frac{1}{\ell - m} \frac{1}{\ell - m} \gamma^\mu \frac{\ell}{(\ell^2 - m^2)} \gamma^\nu L, \\ \lim_{n \rightarrow 4} (\Gamma_{7(e)}^{\text{R5}} - \Gamma_{7(e)}^{\text{BM}}) &= -f^2 g^2 \int \frac{d^n \ell}{(2\pi)^n} \frac{\text{tr}[\ell^2 \ell \gamma^\mu \ell \gamma^\nu L - \ell^2 \ell \gamma^\mu \ell \gamma^\nu L]}{(\ell^2 - m^2)^4} \\ &= -f^2 g^2 \int \frac{d^n \ell}{(2\pi)^n} \frac{\text{tr}[\ell \gamma^\mu \ell_\Delta \gamma^\nu L]}{(\ell^2 - m^2)^3} \\ &= -\frac{1}{(4\pi)^2} if^2 g^2 g^{\mu\nu}.\end{aligned}$$

Exchanges of the two H and of the two A multiply the above amplitude by a factor of 4, i.e., the total amplitude is $-\frac{1}{(4\pi)^2} i4f^2 g^2 g^{\mu\nu}$.

Diagram (f):

$$\begin{aligned}\Gamma_{7(f)}^{\text{BM}} &= -f^2 g^2 \text{tr} \int \frac{d^n \ell}{(2\pi)^n} \frac{1}{\ell - m} \frac{1}{\ell - m} R\gamma^\mu L \frac{1}{\ell - m} \frac{1}{\ell - m} R\gamma^\nu L, \\ \Gamma_{7(f)}^{\text{R5}} &= -f^2 g^2 \text{tr} \int \frac{d^n \ell}{(2\pi)^n} \frac{1}{\ell - m} \frac{1}{\ell - m} \gamma^\mu \frac{2m \ell}{(\ell^2 - m^2)^2} \gamma^\nu L, \\ \lim_{n \rightarrow 4} (\Gamma_{7(f)}^{\text{R5}} - \Gamma_{7(f)}^{\text{BM}}) &= 0.\end{aligned}$$

Diagram (g):

$$\begin{aligned}
 \Gamma_{7(g)}^{\text{BM}} &= f^2 g^2 \text{tr} \int \frac{d^n \ell}{(2\pi)^n} \frac{1}{\ell - m} \gamma_5 \frac{1}{\ell - m} \gamma_5 \frac{1}{\ell - m} R \gamma^\mu L \frac{1}{\ell - m} R \gamma^\nu L, \\
 \Gamma_{7(g)}^{\text{R5}} &= -f^2 g^2 \text{tr} \int \frac{d^n \ell}{(2\pi)^n} \frac{1}{\ell - m} \frac{1}{\ell + m} \frac{1}{\ell - m} \gamma^\mu \frac{\ell}{\ell^2 - m^2} \gamma^\nu L, \\
 \lim_{n \rightarrow 4} (\Gamma_{7(g)}^{\text{R5}} - \Gamma_{7(g)}^{\text{BM}}) &= -f^2 g^2 \int \frac{d^n \ell}{(2\pi)^n} \frac{\text{tr}[\ell^2 \ell \gamma^\mu \ell \gamma^\nu L + \ell \gamma_5 \ell \gamma_5 \ell R \gamma^\mu L \ell R \gamma^\nu L]}{(\ell^2 - m^2)^4} \\
 &= \frac{1}{2} f^2 g^2 \int \frac{d^n \ell}{(2\pi)^n} \frac{\ell_\Delta^2 (\ell^2 + 2\ell^2)}{(\ell^2 - m^2)^4} \text{tr}[\gamma^\mu \gamma^\nu] \\
 &= -\frac{1}{(4\pi)^2} i \frac{7}{3} f^2 g^2 g^{\mu\nu}.
 \end{aligned}$$

Permuting the two external ϕ_2 and the two external A yields three additional diagrams and each of them contributes the same counterterm amplitude as the above. The total counterterm amplitude is therefore equal to $2 \times 2 \times (-\frac{1}{(4\pi)^2} i \frac{7}{3} f^2 g^2 g^{\mu\nu}) = -\frac{1}{(4\pi)^2} i \frac{28}{3} f^2 g^2 g^{\mu\nu}$.

Diagram (h):

$$\Gamma_{7(h)}^{\text{BM}} = f^2 g^2 \text{tr} \int \frac{d^n \ell}{(2\pi)^n} \frac{1}{\ell - m} \gamma_5 \frac{1}{\ell - m} R \gamma^\mu L \frac{1}{\ell - m} \gamma_5 \frac{1}{\ell - m} R \gamma^\nu L.$$

The rightmost- γ_5 amplitude vanishes in the T_0 order;

$$\begin{aligned}
 \Gamma_{7(h)}^{\text{R5}} &= 0, \\
 \lim_{n \rightarrow 4} (\Gamma_{7(h)}^{\text{R5}} - \Gamma_{7(h)}^{\text{BM}}) &= 4f^2 g^2 \text{tr} \int \frac{d^n \ell}{(2\pi)^n} \frac{-\ell_\Delta^2 \ell \gamma^\mu \ell \gamma^\nu L}{(\ell^2 - m^2)^4} \\
 &= 4f^2 g^2 \frac{4}{n(n+2)} \int \frac{d^n \ell}{(2\pi)^n} \frac{(n-4)}{(\ell^2 - m^2)^2} g^{\mu\nu} \\
 &= -\frac{1}{(4\pi)^2} \frac{4}{3} i f^2 g^2 g^{\mu\nu}.
 \end{aligned}$$

By reversing the loop direction, or by exchanging the two external ϕ_2 fields or the two external A fields, we obtain another diagram that also contributes the same counterterm amplitude as the above. The total counterterm amplitude is $2 \times (-\frac{1}{(4\pi)^2} \frac{4}{3} i f^2 g^2 g^{\mu\nu}) = -\frac{1}{(4\pi)^2} \frac{8}{3} i f^2 g^2 g^{\mu\nu}$.

Diagram (i):

$$\begin{aligned}
 \Gamma_{7(i)}^{\text{BM}} &= -g^4 \int \frac{d^n \ell}{(2\pi)^n} \frac{\text{tr}[R \gamma^\mu L \ell R \gamma^\nu L \ell R \gamma^\rho L \ell R \gamma^\sigma L]}{(\ell^2 - m^2)^4}, \\
 \Gamma_{7(i)}^{\text{R5}} &= -g^4 \int \frac{d^n \ell}{(2\pi)^n} \frac{\text{tr}[\ell \gamma^\mu \ell \gamma^\nu \ell \gamma^\rho \ell \gamma^\sigma L]}{(\ell^2 - m^2)^4}, \\
 \lim_{n \rightarrow 4} (\Gamma_{7(i)}^{\text{R5}} - \Gamma_{7(i)}^{\text{BM}}) &= -g^4 \int \frac{d^n \ell}{(2\pi)^n} \frac{\text{tr}[\ell \gamma^\mu \ell \gamma^\nu \ell \gamma^\rho \ell \gamma^\sigma L - \ell \gamma^\mu \ell \gamma^\nu \ell \gamma^\rho \ell \gamma^\sigma L]}{(\ell^2 - m^2)^4} \\
 &= \frac{1}{2} g^4 \int \frac{d^n \ell}{(2\pi)^n} \frac{\ell_\Delta^2 \text{tr}[\ell^2 (-2\gamma^\mu \gamma^\nu \gamma^\rho \gamma^\sigma + \gamma^\mu \gamma^\sigma g^{\nu\rho} + g^{\mu\nu} \gamma^\rho \gamma^\sigma) - \ell_\Delta^2 \gamma^\mu \gamma^\nu \gamma^\rho \gamma^\sigma]}{(\ell^2 - m^2)^4} \\
 &= \frac{1}{(4\pi)^2} i g^4 \left(g^{\mu\nu} g^{\rho\sigma} - \frac{5}{3} g^{\mu\rho} g^{\nu\sigma} + g^{\mu\sigma} g^{\rho\nu} \right). \tag{A2}
 \end{aligned}$$

The above amplitude is invariant if we reverse the loop direction or make the interchange ($\mu \leftrightarrow \sigma$). For the 4-point AAAA 1PI function, there are in total 6 topologically different diagrams that may be obtained from Fig. 7(i) by permuting the indices ν , ρ , and σ . The total amplitude for AAAA is equal to

TABLE X. Counterterms due to diagrams in Fig. 7 are shown in the table.

Figure	$(4\pi)^2 \times (\Gamma^{R5} - \Gamma^{BM})$	Multiplicity	$(4\pi)^2 \times \text{counterterm}$
7(a)	0	3!	0
7(b)	$4if^4$	4	$4f^4 H^2(\phi_2)^2$
7(c)	0	2	0
7(d)	$\frac{32}{3}if^4$	3!	$\frac{8}{3}f^4(\phi_2)^4$
7(e)	$-if^2 g^2 g^{\mu\nu}$	4	$-f^2 g^2 H^2 A^2$
7(f)	0	2	0
7(g)	$-i\frac{2}{3}f^2 g^2 g^{\mu\nu}$	4	$-\frac{2}{3}f^2 g^2(\phi_2)^2 A^2$
7(h)	$-i\frac{4}{3}f^2 g^2 g^{\mu\nu}$	2	$-\frac{2}{3}f^2 g^2(\phi_2)^2 A^2$
7(i) + $(\rho \leftrightarrow \nu) + (\rho \leftrightarrow \sigma)$	$i\frac{8}{3}(g^{\mu\nu}g^{\rho\sigma} + g^{\mu\rho}g^{\nu\sigma} + g^{\mu\sigma}g^{\rho\nu})$	2	$\frac{1}{12}g^4(A^2)^2$

$$\begin{aligned} & \frac{1}{(4\pi)^2} i2g^4 \left(g^{\mu\nu}g^{\rho\sigma} - \frac{5}{3}g^{\mu\rho}g^{\nu\sigma} + g^{\mu\sigma}g^{\rho\nu} + (\rho \leftrightarrow \nu) + (\rho \leftrightarrow \sigma) \right) \\ &= \frac{1}{(4\pi)^2} i\frac{2}{3}g^4 (g^{\mu\nu}g^{\rho\sigma} + g^{\mu\rho}g^{\nu\sigma} + g^{\mu\sigma}g^{\rho\nu}). \end{aligned}$$

To summarize, the amplitudes and finite counterterms due to diagrams in Fig. 7 are tabulated in Table X.

APPENDIX B: THE CHIRAL NON-ABELIAN GAUGE THEORY

1. Feynman rules

The propagators and vertices used in the 1-loop counterterm calculation for the chiral Abelian-Higgs theory defined by (28) are listed below.

a. Propagators

$$S(\psi, \bar{\psi}; p) : \begin{array}{c} \psi \quad p \quad \bar{\psi} \\ \xrightarrow{\quad} \xleftarrow{\quad} \end{array} = \frac{i}{\not{p}}$$

$$S(\psi', \bar{\psi}'; p) : \begin{array}{c} \psi' \quad p \quad \bar{\psi}' \\ \xrightarrow{\quad} \xleftarrow{\quad} \end{array} = \frac{i}{\not{p}}$$

$$D(A^{a,\mu}, A^{b,\nu}; k) : \begin{array}{c} \leftarrow k \\ a, \mu \quad \text{wavy line} \quad b, \nu \end{array} = \frac{-i}{k^2} \left(g^{\mu\nu} + (\alpha - 1) \frac{k^\mu k^\nu}{k^2} \right) \delta^{ab}$$

b. Vertex factors

$$\bar{\psi} A^{a,\mu} \psi : \begin{array}{c} \text{wavy line } A^{a,\mu} \\ \leftarrow \quad \rightarrow \\ \bar{\psi} \quad \psi \end{array} = -igR\gamma^\mu L T_L^a$$

$$\bar{\psi}' A^{a,\mu} \psi' : \begin{array}{c} \text{wavy line } A^{a,\mu} \\ \leftarrow \quad \rightarrow \\ \bar{\psi}' \quad \psi' \end{array} = -igL\gamma^\mu R T_R^a$$

$$A_\mu^a A_\nu^b A_\rho^c : \begin{array}{c} A^{a,\mu} \\ \downarrow k_1 \\ \text{wavy line } A^{a,\mu} \\ \swarrow \quad \searrow \\ A^{b,\nu} \quad A^{c,\rho} \\ \nearrow \quad \nwarrow \\ k_2 \quad k_3 \end{array}$$

$$= -gC^{abc} (g^{\mu\nu} (k_1 - k_2)^\rho + g^{\nu\rho} (k_2 - k_3)^\mu + g^{\mu\rho} (k_3 - k_1)^\nu)$$

2. 1-Loop counterterms
a. Figure 8: Fermion self-energy diagram

The fermion field in Fig. 8 can be either ψ or ψ' . If the fermion field is ψ , the Feynman integral for Fig. 8 without including the non-Abelian group factor $\sum_e T_L^e T_L^e = C_L$ is the same as the one for the diagram of (14) of which the counterterm has been demonstrated to be (19) in Sec. IV. If the fermion field is ψ' , the counterterm can be obtained from that for the ψ field by replacing γ_5 with $-\gamma_5$ and the group factor C_L with $\sum_e T_R^e T_R^e = C_R$. The counterterm therefore is equal to

$$-\frac{1}{(4\pi)^2} \frac{1}{3} g^2 (1 + 2\alpha) (\bar{\psi}_L i \not{\partial} \psi_L C_L + \bar{\psi}'_R i \not{\partial} \psi'_R C_R). \quad (\text{B1})$$

b. Figure 9: $\bar{\psi} A \psi$ and $\bar{\psi}' A \psi'$ Vertex diagrams

Diagram (a):

The amplitude for this diagram excluding the non-Abelian group factor is the same as that for Fig. 2(a). If ψ is the fermion field, the non-Abelian group factor is $\sum_e T_L^e T_L^e T_L^e = C_L T_L^a + iC^{abc} T_L^b T_L^c$ and

$$\lim_{n \rightarrow 4} (\Gamma_{\psi,9(a)}^{\text{R5}} - \Gamma_{\psi,9(a)}^{\text{BM}}) = \frac{1}{(4\pi)^2} \frac{ig^3}{6} (7 + 5\alpha) \times \gamma^\mu L (C_L T_L^a + iC^{abc} T_L^b T_L^c). \quad (\text{B2})$$

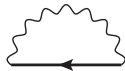


FIG. 8. The fermion self-energy diagram is shown.

If ψ' is the fermion field, the non-Abelian group factor is $\sum_e T_R^e T_R^e T_R^e = C_R T_R^a + iC^{abc} T_R^b T_R^c$ and

$$\lim_{n \rightarrow 4} (\Gamma_{\psi',9(a)}^{\text{R5}} - \Gamma_{\psi',9(a)}^{\text{BM}}) = \frac{1}{(4\pi)^2} \frac{ig^3}{6} (7 + 5\alpha) \times \gamma^\mu R (C_R T_R^a + iC^{abc} T_R^b T_R^c). \quad (\text{B3})$$

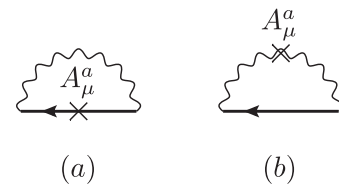
The counterterm that is responsible for the amplitudes of (B2) and (B3) is

$$\frac{1}{6} g^3 (7 + 5\alpha) \bar{\psi}_L A^a (C_L T_L^a + iC^{abc} T_L^b T_L^c) \psi_L + \frac{1}{6} g^3 (7 + 5\alpha) \bar{\psi}'_R A^a (C_R T_R^a + iC^{abc} T_R^b T_R^c) \psi'_R. \quad (\text{B4})$$

Diagram (b):

If ψ is the fermion field, we have

$$\Gamma_{\psi,9(b)}^{\text{BM}} = -ig^3 \lim_{m \rightarrow 0} \int \frac{d^n \ell}{(2\pi)^n} R \gamma^\tau L \times \frac{1}{\ell - m} R \gamma^\sigma L C^{bac} T_L^b T_L^c D_{\tau\nu}(\ell - k_1) \times (2g^{\nu\rho} 2\ell^\mu - g^{\mu\nu} \ell^\rho - g^{\mu\rho} \ell^\nu) D_{\rho\sigma}(\ell),$$


 FIG. 9. $\bar{\psi} A \psi$ and $\bar{\psi}' A \psi'$ vertex diagrams are shown.

and

$$\begin{aligned}
& \lim_{n \rightarrow 4} (\Gamma_{\psi,9(b)}^{\text{R5}} - \Gamma_{\psi,9(b)}^{\text{BM}}) \\
&= -ig^3 \lim_{m \rightarrow 0} \int \frac{d^n \ell}{(2\pi)^n} D_{\tau\nu}(\ell) (2g^{\nu\rho} 2\ell^\mu - g^{\mu\nu} \ell^\rho - g^{\mu\rho} \ell^\nu) \\
&\quad \times D_{\rho\sigma}(\ell) \frac{1}{\ell^2 - m^2} (\gamma^\tau \ell \gamma^\sigma - \underline{\gamma^\tau \ell \gamma^\sigma}) LC^{bac} T_L^b T_L^c \\
&= \frac{1}{(4\pi)^2} \frac{1}{6} (7 + 5\alpha) g^3 \gamma^\mu LC^{abc} T_L^b T_L^c. \tag{B5}
\end{aligned}$$

If ψ' is the fermion field, we have

$$\begin{aligned}
\Gamma_{\psi',9(b)}^{\text{BM}} &= -ig^3 \lim_{m \rightarrow 0} \int \frac{d^n \ell}{(2\pi)^n} L \gamma^\tau R \\
&\quad \times \frac{1}{\ell - m} L \gamma^\sigma RC^{bac} T_R^b T_R^c D_{\tau\nu}(\ell - k_1) \\
&\quad \times (2g^{\nu\rho} 2\ell^\mu - g^{\mu\nu} \ell^\rho - g^{\mu\rho} \ell^\nu) D_{\rho\sigma}(\ell)
\end{aligned}$$

and

$$\begin{aligned}
& \lim_{n \rightarrow 4} (\Gamma_{\psi',9(b)}^{\text{R5}} - \Gamma_{\psi',9(b)}^{\text{BM}}) \\
&= -ig^3 \lim_{m \rightarrow 0} \int \frac{d^n \ell}{(2\pi)^n} D_{\tau\nu}(\ell) \\
&\quad \times (2g^{\nu\rho} 2\ell^\mu - g^{\mu\nu} \ell^\rho - g^{\mu\rho} \ell^\nu) D_{\rho\sigma}(\ell) \\
&\quad \times \frac{1}{\ell^2 - m^2} (\gamma^\tau \ell \gamma^\sigma - \underline{\gamma^\tau \ell \gamma^\sigma}) RC^{bac} T_R^b T_R^c \\
&= \frac{1}{(4\pi)^2} \frac{1}{6} (7 + 5\alpha) g^3 \gamma^\mu RC^{abc} T_R^b T_R^c. \tag{B6}
\end{aligned}$$

The counterterm to generate the amplitudes of (B5) and (B6) is

$$\begin{aligned}
& -i \frac{1}{(4\pi)^2} \frac{1}{6} g^3 (7 + 5\alpha) (\bar{\psi}_L A^a C^{abc} T_L^b T_L^c \psi_L \\
&+ \bar{\psi}'_R A^a C^{abc} T_R^b T_R^c \psi'_R). \tag{B7}
\end{aligned}$$

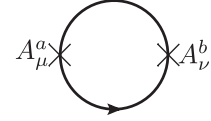


FIG. 10. The diagram for 2-point 1PI is shown.

To summarize, the sum of (B4) and (B7) is the total counterterm due to the two diagrams in Fig. 9:

$$\frac{1}{(4\pi)^2} \frac{1}{6} g^3 (7 + 5\alpha) (\bar{\psi}_L A^a T_L^a \psi_L C_L + \bar{\psi}'_R A^a T_R^a \psi'_R C_R). \tag{B8}$$

c. Figure 10: One-fermion-loop 2-point 1PI

Ignoring the non-Abelian group factor, the diagram in Fig. 10 is the same as diagram (c) in Fig. 5. For the ψ fermion field, the group factor is $\text{tr}(T_L^a T_L^b) = T_L \delta^{ab}$. Consequently,

$$\lim_{n \rightarrow 4} (\Gamma_{\psi,10}^{\text{R5}} - \Gamma_{\psi,10}^{\text{BM}}) = \frac{1}{(4\pi)^2} ig^{\mu\nu} \frac{1}{3} g^2 p^2 T_L \delta^{ab},$$

where p is the external momentum. The group factor for ψ' is $\text{tr}(T_R^a T_R^b) = T_R \delta^{ab}$ which yields the difference

$$\lim_{n \rightarrow 4} (\Gamma_{\psi',10}^{\text{R5}} - \Gamma_{\psi',10}^{\text{BM}}) = \frac{1}{(4\pi)^2} ig^{\mu\nu} \frac{1}{3} g^2 p^2 T_R \delta^{ab}.$$

The above two amplitudes can be accounted for by the counterterm

$$-\frac{1}{(4\pi)^2} \frac{1}{6} g^2 (T_L + T_R) A_\mu^a \square A^{a,\mu}. \tag{B9}$$

d. Figure 11: One-fermion-loop 3-point 1PI

We are only interested in terms that have an even count of γ_5 . Assume the incoming momenta entering $A_\mu^a, A_\nu^b, A_\rho^c$ are k_1, k_2, k_3 .

Diagram (a):

$$\begin{aligned}
\Gamma_{\psi,11(a)}^{\text{BM}} &= -g^3 \lim_{m \rightarrow 0} \text{tr} \int \frac{d^n \ell}{(2\pi)^n} \left(\frac{1}{\ell - m} R \gamma^\mu L \frac{1}{\ell - k_1 - m} R \gamma^\nu L \frac{1}{\ell + k_3 - m} R \gamma^\rho L \right)_{\gamma_5\text{-even}} \text{tr}(T^a T^b T^c), \\
\lim_{n \rightarrow 4} (\Gamma_{\psi,11(a)}^{\text{R5}} - \Gamma_{\psi,11(a)}^{\text{BM}}) &= -\frac{g^3}{2} \lim_{m \rightarrow 0} \int \frac{d^n \ell}{(2\pi)^n} \frac{\text{tr}(\ell \gamma^\mu (\ell - k_1) \gamma^\nu (\ell + k_3) \gamma^\rho - \ell \gamma^\mu (\ell - k_1) \gamma^\nu (\ell + k_3) \gamma^\rho)}{(\ell^2 - m^2)((\ell - k_1)^2 - m^2)((\ell + k_3)^2 - m^2)} \text{tr}(T^a T^b T^c) \\
&= -\frac{1}{(4\pi)^2} \frac{2i}{3} g^3 ((k_2 - k_3)^\mu g^{\nu\rho} + (k_3 - k_1)^\nu g^{\mu\rho} + (k_1 - k_2)^\rho g^{\mu\nu}) \text{tr}(T_L^a T_L^b T_L^c). \tag{B10}
\end{aligned}$$

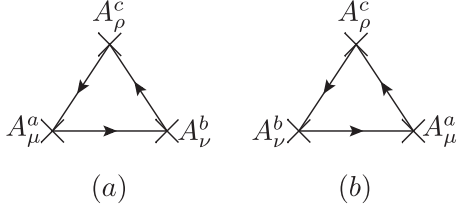


FIG. 11. The diagrams for 3-point 1PI are shown.

Similarly,

$$\begin{aligned} & \lim_{n \rightarrow 4} (\Gamma_{\psi', 11(a)}^{\text{RS}} - \Gamma_{\psi', 11(a)}^{\text{BM}}) \\ &= -\frac{1}{(4\pi)^2} \frac{2i}{3} g^3 ((k_2 - k_3)^\mu g^{\nu\rho} + (k_3 - k_1)^\nu g^{\mu\rho} \\ &+ (k_1 - k_2)^\rho g^{\mu\nu}) \text{tr}(T_R^a T_R^b T_R^c). \end{aligned} \quad (\text{B11})$$

Diagram (b):

Diagram (b) can be obtained from diagram (a) by the interchange $(a, \mu, k_1) \leftrightarrow (b, \nu, k_2)$

$$\begin{aligned} & \lim_{n \rightarrow 4} (\Gamma_{\psi, 11(b)}^{\text{RS}} - \Gamma_{\psi, 11(b)}^{\text{BM}}) \\ &= \frac{1}{(4\pi)^2} \frac{2i}{3} g^3 ((k_2 - k_3)^\mu g^{\nu\rho} + (k_3 - k_1)^\nu g^{\mu\rho} \\ &+ (k_1 - k_2)^\rho g^{\mu\nu}) \text{tr}(T_L^a T_L^b T_L^c), \end{aligned} \quad (\text{B12})$$

$$\begin{aligned} & \lim_{n \rightarrow 4} (\Gamma_{\psi', 11(b)}^{\text{RS}} - \Gamma_{\psi', 11(b)}^{\text{BM}}) \\ &= \frac{1}{(4\pi)^2} \frac{2i}{3} g^3 ((k_2 - k_3)^\mu g^{\nu\rho} + (k_3 - k_1)^\nu g^{\mu\rho} \\ &+ (k_1 - k_2)^\rho g^{\mu\nu}) \text{tr}(T_R^b T_R^a T_R^c). \end{aligned} \quad (\text{B13})$$

Utilizing $\text{tr}([T_L^a, T_L^b] T_L^c) = iT_L C^{abc}$ and $\text{tr}([T_R^a, T_R^b] T_R^c) = iT_R C^{abc}$, the summation from (B10) to (B13) can be written as

$$\begin{aligned} & \frac{1}{(4\pi)^2} \frac{2}{3} g^3 ((k_2 - k_3)^\mu g^{\nu\rho} + (k_3 - k_1)^\nu g^{\mu\rho} \\ &+ (k_1 - k_2)^\rho g^{\mu\nu}) C^{abc} (T_L + T_R), \end{aligned}$$

which leads to the counterterm

$$-\frac{1}{(4\pi)^2} \frac{2}{3} g^3 (T_L + T_R) C^{abc} (\partial^\mu A_\nu^a) A_\mu^b A^{c,\nu}. \quad (\text{B14})$$

e. Figure 12: One-fermion-loop 4-point 1PI

Diagram (a):

If ψ is the fermion field, the amplitude for this diagram is equal to the group factor $\text{tr}(T_L^a T_L^b T_L^c T_L^d) = T_L^{abcd}$ times the amplitude for diagram (i) in Fig. 7. According to (A2), we then have

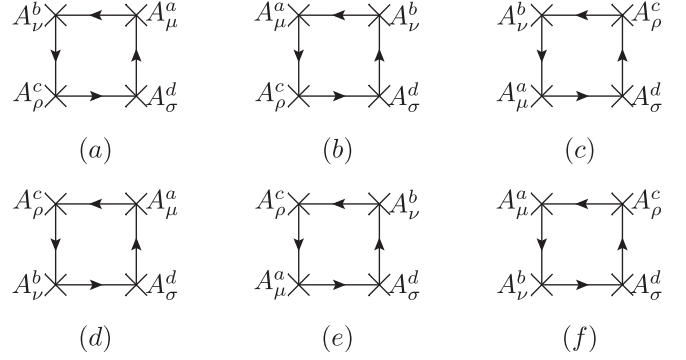


FIG. 12. The diagrams for 4-point 1PI are shown.

$$\begin{aligned} & \lim_{n \rightarrow 4} (\Gamma_{\psi, 12(a)}^{\text{RS}} - \Gamma_{\psi, 12(a)}^{\text{BM}}) \\ &= \frac{1}{(4\pi)^2} i g^4 T_L^{abcd} \left(g^{\mu\nu} g^{\rho\sigma} - \frac{5}{3} g^{\mu\rho} g^{\nu\sigma} + g^{\mu\sigma} g^{\nu\rho} \right). \end{aligned} \quad (\text{B15})$$

Likewise, if ψ' is the fermion field, $\text{tr}(T_R^a T_R^b T_R^c T_R^d) = T_R^{abcd}$ is the group factor and

$$\begin{aligned} & \lim_{n \rightarrow 4} (\Gamma_{\psi', 12(a)}^{\text{RS}} - \Gamma_{\psi', 12(a)}^{\text{BM}}) \\ &= \frac{1}{(4\pi)^2} i g^4 T_R^{abcd} \left(g^{\mu\nu} g^{\rho\sigma} - \frac{5}{3} g^{\mu\rho} g^{\nu\sigma} + g^{\mu\sigma} g^{\nu\rho} \right). \end{aligned} \quad (\text{B16})$$

The contribution to the difference from both ψ and ψ' fermion loops is the sum of (B15) and (B16), which is equal to

$$\begin{aligned} & \lim_{n \rightarrow 4} (\Gamma_{12(a)}^{\text{RS}} - \Gamma_{12(a)}^{\text{BM}}) \\ &= \frac{1}{(4\pi)^2} i g^4 (T_L^{abcd} + T_R^{abcd}) \\ &\times \left(g^{\mu\nu} g^{\rho\sigma} - \frac{5}{3} g^{\mu\rho} g^{\nu\sigma} + g^{\mu\sigma} g^{\nu\rho} \right). \end{aligned} \quad (\text{B17})$$

Diagram (b):

The interchange $(a, \mu) \leftrightarrow (b, \nu)$ on (B17) yields

$$\begin{aligned} & \lim_{n \rightarrow 4} (\Gamma_{12(b)}^{\text{RS}} - \Gamma_{12(b)}^{\text{BM}}) \\ &= \frac{1}{(4\pi)^2} i g^4 (T_L^{bacd} + T_R^{bacd}) \\ &\times \left(g^{\mu\nu} g^{\rho\sigma} + g^{\mu\rho} g^{\nu\sigma} - \frac{5}{3} g^{\mu\sigma} g^{\nu\rho} \right). \end{aligned} \quad (\text{B18})$$

TABLE XI. Counterterms due to diagrams in Figs. 8–12 are shown in the table.

Figure	Where	$(4\pi)^2 \times \text{counterterm}$
8	(B1)	$-\frac{1}{3}g^2(1+2\alpha)(\bar{\psi}_L i \not{\partial} \psi_L C_L + \bar{\psi}'_R i \not{\partial} \psi'_R C_R)$
9	(B8)	$\frac{1}{6}g^3(7+5\alpha)(\bar{\psi}_L A^a T_L^a \psi_L C_L + \bar{\psi}'_R A^a T_R^a \psi'_R C_R)$
10	(B9)	$-\frac{1}{6}g^2(T_L + T_R)A_\mu^a \square A^{a,\mu}$
11	(B14)	$-\frac{2}{3}g^3(T_L + T_R)C^{abc}(\partial^\mu A_\nu^a)A_\mu^b A^{c,\nu}$
12	(B24)	$(\frac{1}{12}g^4(T_L^{abcd} + T_R^{abcd})A^{a,\mu}A_\mu^b A^{c,\nu}A_\nu^d + \frac{5}{24}g^4(T_L + T_R)C^{eab}C^{ecd}A_\mu^a A_\nu^b A^{c,\mu}A^{d,\nu})$

Diagram (c):

The interchange $(a, \mu) \leftrightarrow (c, \rho)$ on (B17) yields

$$\begin{aligned} & \lim_{n \rightarrow 4} (\Gamma_{12(c)}^{R5} - \Gamma_{12(c)}^{BM}) \\ &= \frac{1}{(4\pi)^2} i g^4 (T_L^{cbad} + T_R^{cbad}) \\ & \times \left(g^{\mu\nu} g^{\rho\sigma} - \frac{5}{3} g^{\mu\rho} g^{\nu\sigma} + g^{\mu\sigma} g^{\nu\rho} \right). \end{aligned} \quad (\text{B19})$$

Diagram (d):

The interchange $(b, \nu) \leftrightarrow (c, \rho)$ on (B17) yields

$$\begin{aligned} & \lim_{n \rightarrow 4} (\Gamma_{12(d)}^{R5} - \Gamma_{12(d)}^{BM}) \\ &= \frac{1}{(4\pi)^2} i g^4 (T_L^{acbd} + T_R^{acbd}) \\ & \times \left(-\frac{5}{3} g^{\mu\nu} g^{\rho\sigma} + g^{\mu\rho} g^{\nu\sigma} + g^{\mu\sigma} g^{\nu\rho} \right). \end{aligned} \quad (\text{B20})$$

Diagram (e):

The interchange $(b, \nu) \leftrightarrow (c, \rho)$ on (B19) yields

$$\begin{aligned} & \lim_{n \rightarrow 4} (\Gamma_{12(e)}^{R5} - \Gamma_{12(e)}^{BM}) \\ &= \frac{1}{(4\pi)^2} i g^4 (T_L^{bcad} + T_R^{bcad}) \\ & \times \left(-\frac{5}{3} g^{\mu\nu} g^{\rho\sigma} + g^{\mu\rho} g^{\nu\sigma} + g^{\mu\sigma} g^{\nu\rho} \right). \end{aligned} \quad (\text{B21})$$

Diagram (f):

The interchange $(a, \mu) \leftrightarrow (c, \rho)$ on (B20) yields

$$\begin{aligned} & \lim_{n \rightarrow 4} (\Gamma_{12(f)}^{R5} - \Gamma_{12(f)}^{BM}) \\ &= \frac{1}{(4\pi)^2} i g^4 (T_L^{cabd} + T_R^{cabd}) \\ & \times \left(g^{\mu\nu} g^{\rho\sigma} + g^{\mu\rho} g^{\nu\sigma} - \frac{5}{3} g^{\mu\sigma} g^{\nu\rho} \right). \end{aligned} \quad (\text{B22})$$

The summation from (B17) to (B22) gives

$$\frac{1}{(4\pi)^2} i g^4 \left(\begin{aligned} & g^{\mu\nu} g^{\rho\sigma} ((T_{L+R}^{abcd} + T_{L+R}^{bacd} + T_{L+R}^{cbad} + T_{L+R}^{cabd}) - \frac{5}{3} (T_{L+R}^{acbd} + T_{L+R}^{bcad})) \\ & + g^{\mu\rho} g^{\nu\sigma} ((T_{L+R}^{bacd} + T_{L+R}^{cabd} + T_{L+R}^{acbd} + T_{L+R}^{bcad}) - \frac{5}{3} (T_{L+R}^{abcd} + T_{L+R}^{cbad})) \\ & + g^{\mu\sigma} g^{\nu\rho} ((T_{L+R}^{abcd} + T_{L+R}^{cbad} + T_{L+R}^{acbd} + T_{L+R}^{bcad}) - \frac{5}{3} (T_{L+R}^{bacd} + T_{L+R}^{cabd})) \end{aligned} \right), \quad (\text{B23})$$

where $T_{L+R}^{abcd} = T_L^{abcd} + T_R^{abcd}$. The above amplitude can be accounted for by the counterterm

$$\begin{aligned} & \frac{1}{(4\pi)^2} g^4 \left(\frac{1}{2} T_{L+R}^{abcd} A^{a,\mu} A_\mu^b A^{c,\nu} A_\nu^d - \frac{5}{12} T_{L+R}^{abcd} A^{a,\mu} A^{b,\nu} A_\mu^c A_\nu^d \right) \\ &= \frac{1}{(4\pi)^2} g^4 \left(\frac{1}{12} T_{L+R}^{abcd} A^{a,\mu} A_\mu^b A^{c,\nu} A_\nu^d \right. \\ & \left. + \frac{5}{24} (T_L + T_R) C^{eab} C^{ecd} A_\mu^a A_\nu^b A^{c,\mu} A^{d,\nu} \right). \end{aligned} \quad (\text{B24})$$

f. One-loop counterterms for the non-Abelian theory

The results for the finite counterterms stemming from the difference of amplitudes between the rightmost scheme and the BM scheme calculated for the diagrams in Fig. 8–12 in the chiral non-Abelian gauge theory are summarized in Table XI.

- [1] G. 't Hooft and M. Veltman, *Nucl. Phys.* **B44**, 189 (1972).
- [2] P. Breitenlohner and D. Maison, *Commun. Math. Phys.* **52**, 11 (1977).
- [3] J. C. Ward, *Phys. Rev.* **78**, 182 (1950); Y. Takahashi, *Nuovo Cimento* **6**, 371 (1957).
- [4] C. Becchi, A. Rouet, and R. Stora, *Phys. Lett. B* **52**, 344 (1974); *Commun. Math. Phys.* **42**, 127 (1975); *Ann. Phys. (N.Y.)* **98**, 287 (1976); I. V. Tyutin, Lebedev Institute Report No. 39, 1975.
- [5] Guy Bonneau, *Nucl. Phys.* **B177**, 523 (1981).
- [6] R. Ferrari, A. Le Yaouanc, L. Oliver, and J. C. Raynal, *Phys. Rev. D* **52**, 3036 (1995).
- [7] R. Ferrari and P. A. Grassi, *Phys. Rev. D* **60**, 065010 (1999).
- [8] C. P. Martin and D. Sanchez-Ruiz, *Nucl. Phys.* **B572**, 387 (2000).
- [9] D. Sanchez-Ruiz, *Phys. Rev. D* **68**, 025009 (2003).
- [10] E. C. Tsai, *Phys. Rev. D* **83**, 025020 (2011).